# SUPPORTING INFORMATION

# TNF and IL-10 are major factors in modulation of the phagocytic cell environment in lung and lymph node in tuberculosis: a next generation two compartment model

Simeone Marino[1], Amy Myers[2], JoAnne L. Flynn[2], Denise E. Kirschner[1,3]

[1] Department of Microbiology and Immunology, University of Michigan Medical School, Ann Arbor, MI - USA. [2] Department of Microbiology and Molecular Genetics, University of Pittsburgh School of Medicine, Pittsburgh, PA – USA.

[3] Corresponding author: kirschne@umich.edu

## 1. Two compartmental mathematical model

Our two-compartmental model comprises 32 equations with 210 parameters Bacteria are not modeled explicitly: since we have precise available data for the dynamics of the bacteria populations, we use the time courses of bacteria as input functions for the model in the lung (CFUlung) and in the lymph node (CFUln). The remaining equations in the system of non-linear ODE model comprise macrophage (resting, infected, classical and alternatively activated) and dendritic cell (immature and mature) populations in both the lung and lymph node. Naïve CD4+ and naïve CD8+ T cells are also included: they are primed in the lymph node and migrate out to the site of infection as both precursor or effector T helper cells and precursor or effector CTL. These cells elicit their effector functions at the site of infection (lung) after becoming fully differentiated. Cytokines (TNF, IFNγ, IL10 and IL12) are also explicitly modeled, both in the lung and the lymph node. Table 1 in the main manuscript describes all the variables in the model. We list here all the differential equations and most of the diagrams of cell dynamics.

### *1.1. Macrophage equations in the Lung*

Below are the equations described macrophage dynamics in the lung and in the lymph node. A diagram of macrophage dynamics is shown in the main manuscript (Figure 1).

*Resting (uncommitted) Macrophages* $(M_0)$

$M_0$ turnover and recruitment

$$\frac{dM_0}{dt} = \left[ s_{M_0} + rc_1 \left( \frac{(M_A + w_1 M_I)}{(M_A + w_1 M_I) + hs_{r1}} \right) + rc_2 \left( \frac{F_\alpha}{F_\alpha + hs_{r2}} \right) \right] - \mu_{M_0} M_0 - k_2 \delta M_0 - k_7 (1-\delta) M_0 \quad (1)$$

Classical $M_{I0}$ activation→CAM; Alternative $M_0$ activation; $M_0$ death

*Infected Macrophages* $(M_I)$

Bursting; FAS apoptosis

$$\frac{dM_I}{dt} = k_1 M_2 \, CFUlung - k_3 M_I \left( \frac{CFUlung^2}{CFUlung^2 + (NM_I)^2} \right) - k_4 M_I \left( \frac{T_1}{T_1 + hs_4} \right) - k_5 M_I \left( \frac{F_\alpha}{F_\alpha + hs_5} \right) - k_6 M_I \left( \frac{T_C}{T_C + hs_6} \right) - \mu_{M_I} M_I \quad (2)$$

$M_2$ infection due to bacterial uptake; TNF apoptosis; $M_I$ death; CTL killing

*Classically Activated Macrophages* $(M_A \ or \ M_1)$

$$\frac{dM_A}{dt} = k_2 \delta M_0 - k_5 M_A \left( \frac{F_\alpha}{F_\alpha + hs_5} \right) - \mu_{M_A} M_A + k_{21} \delta M_2 \quad (3)$$

CAM differentiation (from $M_0$); TNF apoptosis; $M_A$ death; CAM differentiation (from $M_2$)

*Alternatively Activated Macrophages* $(M_2)$

$$\frac{dM_2}{dt} = k_7 (1-\delta) M_0 - k_1 M_2 CFUlung - k_5 M_2 \left( \frac{F_\alpha}{F_\alpha + hs_5} \right) - \mu_{M_2} M_2 - k_{21} \delta M_2 \quad (4)$$

$M_2$ differentiation (from $M_0$); $M_2$ infection due to bacterial uptake; TNF apoptosis; $M_A$ death; $M_2$ differentiation (to CAM)

where

$$\delta = \left( \frac{I_\gamma}{I_\gamma + hs_2} \right) \left( \frac{CFUlung + f_1 F_\alpha}{CFUlung + f_1 F_\alpha + hs_3} \right) \left( 1 - \frac{I_{10}}{I_{10} + hs_{I_{10}}} \right)$$

### *1.2. Macrophage dynamics in the Lymph Node*

*Resting (uncommitted) Macrophages* $\left(M_0^{LN}\right)$

$$\frac{dM_0^{LN}}{dt}=\left[s_{m_{0a}}+rc_{1a}\left(\frac{(M_A^{LN}+w_1M_I^{LN})}{(M_A^{LN}+w_1M_I^{LN})+hs_{r1a}}\right)+rc_{2a}\left(\frac{F_\alpha^{LN}}{F_\alpha^{LN}+hs_{r2a}}\right)\right]-\mu_{M_0}M_0^{LN}- \quad (5)$$
$$-k_{2a}\delta_{LN}M_0^{LN}-k_{7a}(1-\delta_{LN})M_0^{LN}$$

$M_0$ turnover and recruitment; $M_0$ death; Classical $M_{I0}$ activation→CAM; Alternative $M_0$ activation

*Infected Macrophages* $\left(M_I^{LN}\right)$

$$\frac{dM_I^{LN}}{dt}=k_{1a}M_2^{LN}CFU\ln-k_{3a}M_I^{LN}\left(\frac{(CFU\ln)^2}{(CFU\ln)^2+(NM^{LN})^2}\right)-k_{4a}M_I^{LN}\left(\frac{T_1^{LN}}{T_1^{LN}+hs_{4a}}\right)- \quad (6)$$
$$-k_{5a}M_I^{LN}\left(\frac{F_\alpha^{LN}}{F_\alpha^{LN}+hs_{5a}}\right)-k_{6a}M_I^{LN}\left(\frac{T_C^{LN}}{T_C^{LN}+hs_{6a}}\right)-\mu_{M_I}M_I^{LN}$$

Bursting; FAS apoptosis; $M_2$ infection due to bacterial uptake; TNF apoptosis; CTL killing; $M_I$ death

*Classically Activated Macrophages* $\left(M_A^{LN}\right)$

$$\frac{dM_A^{LN}}{dt}=k_{2a}\delta_{LN}M_0^{LN}-k_{5a}M_A^{LN}\left(\frac{F_\alpha^{LN}}{F_\alpha^{LN}+hs_{5a}}\right)-\mu_{M_A}M_A^{LN}+k_{21a}\delta_{LN}M_2^{LN} \quad (7)$$

$M_A$ differentiation (from $M_0$); TNF apoptosis; $M_A$ death; CAM differentiation (from $M_2$)

*Alternatively Activated Macrophages* $\left(M_2^{LN}\right)$

$$\frac{dM_2^{LN}}{dt}=k_{7a}(1-\delta_{LN})M_0^{LN}-k_{1a}M_2^{LN}CFU\ln-k_{5a}M_2^{LN}\left(\frac{F_\alpha^{LN}}{F_\alpha^{LN}+hs_{5a}}\right)-\mu_{M_2}M_2^{LN}-k_{21a}\delta_{LN}M_2^{LN} \quad (8)$$

$M_2$ differentiation (from $M_0$); $M_2$ infection due to bacterial uptake; TNF apoptosis; $M_2$ death; $M_2$ differentiation (to CAM)

where

$$\delta_{LN}=\left(\frac{I_\gamma^{LN}}{I_\gamma^{LN}+hs_{2a}}\right)\left(\frac{CFU\ln+f_1F_\alpha^{LN}}{CFU\ln+f_1F_\alpha^{LN}+hs_{3a}}\right)\left(1-\frac{I_{10}^{LN}}{I_{10}^{LN}+hs_{I_{10a}}}\right)$$

### *1.3. Dendritic Cell Dynamics in the Lung and Lymph Node*

A diagram of dendritic cell dynamics in both compartments is shown in Figure S2. Below are the equations. We model two types of dendritic cell populations in each compartment: immature dendritic cells (IDCs) and mature dendritic cells (MDCs) (see Supporting Information online for the equations). Equation (9) represents the IDCs in the lung, describing a constant source $s_{IDC}$ as well as both TNF-independent ($rc_3$ term) and TNF-dependent ($rc_4$ term) recruitment. Loss of IDCs is modeled with IDC uptake of bacteria (resulting in DC maturation, $k_{12}$ term) or death at a rate of $\mu_{IDC}$. DC uptake and maturation is delayed by the action of IL10 [1]. Equation (10) describes MDCs in the lung, showing a balance between IDC uptake of bacteria (production of MDCs) and MDC migration to the lymph node ($\varphi$).The equations for the lymph node are similar to those for the lung. Equation (11) describes IDCs in the lymph node, once again including a constant source term, TNF-independent and TNF-dependent recruitment, IDC uptake of bacteria, and death. DC maturation includes MDC equation for the lymph node (equation (12)) includes IDC migration from the lung $\varphi MDC_L/\Upsilon$ (where $\Upsilon$ represents a scaling factor between the lung and the lymph node), the exosome mechanism, which is captured by the $k_{12b}$ term [2,3,4].

*Immature DC in the lung* $(IDC)$

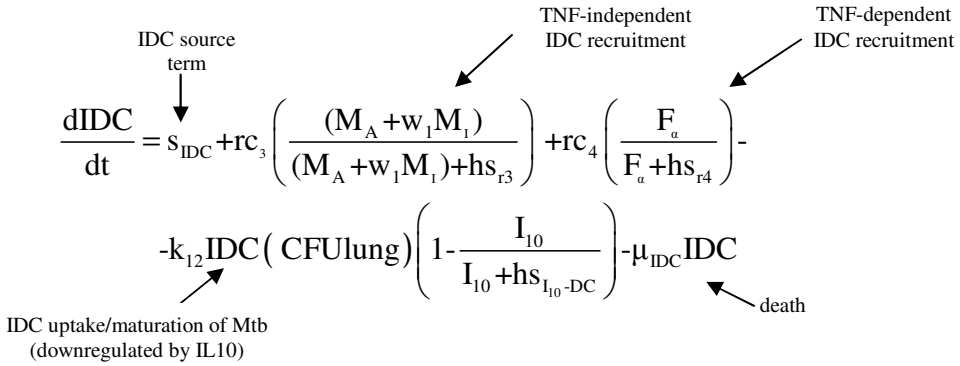


(9)

*Mature DC in the Lung* $(MDC_L)$

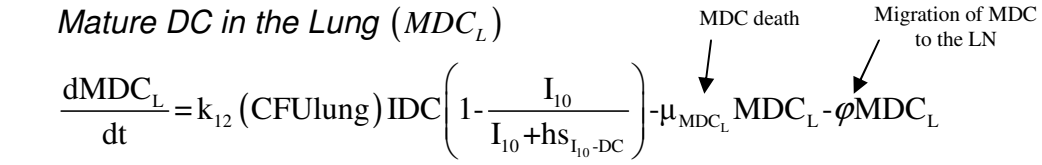


(10)

*Immature DC in the lymph node* $(IDC_{LN})$

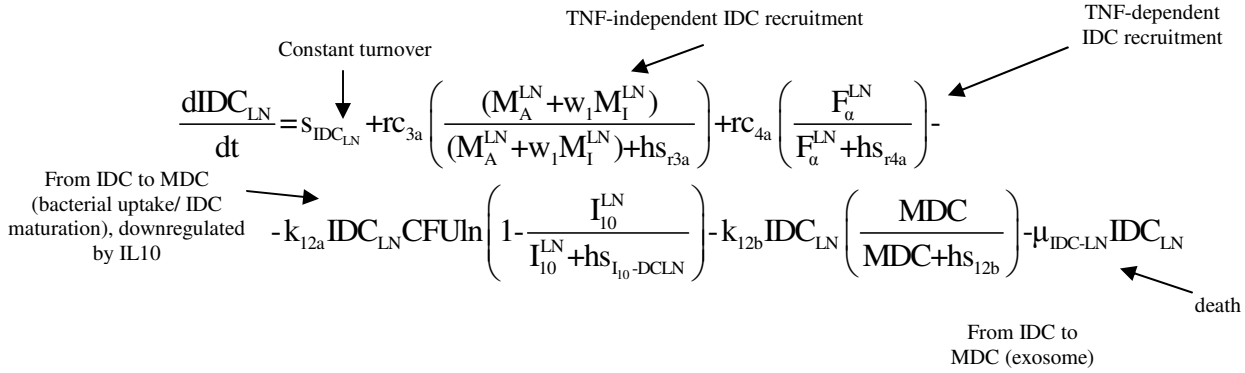


(11)

*Mature DC in the lymph node* $(MDC)$

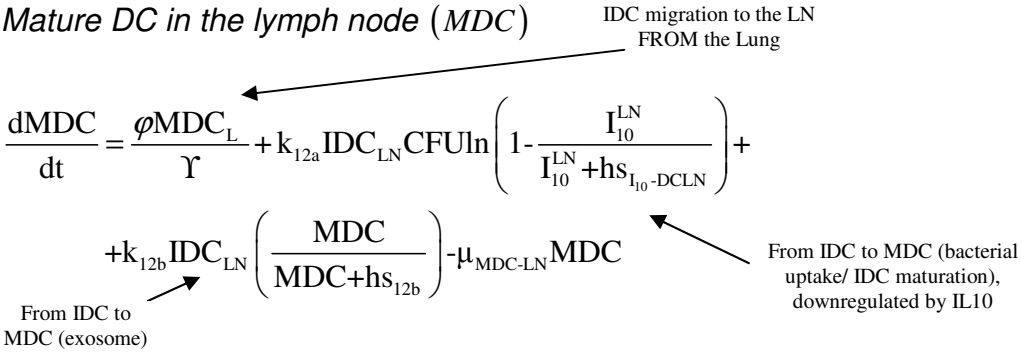


(12)

### *1.4. Lymphocytes Dynamics in the Lymph Node (LN)*

A diagram of lymph node dynamics is shown in Figure S3. Below are the equations. We model lymphocytes in both the lymph node and lung. In the lymph node, naïve CD4+ T cells are described in equation (13) with a constant source term ($s_{N4}$), recruitment by a MDC-dependent recruitment term ($k_{13}$ term), natural death, and differentiation to precursor Th1 that depends on MDCs ($k_{14}$ term). Equation (14) models precursor Th1 cell dynamics. It accounts for the differentiation of naïve CD4+ T cells, proliferation of Th1 cells (logistic growth with rate constant $k_{15}$, with IL10 down-regulation), differentiation, and migration into the blood ($\xi_1$ term).Equation (15) describes Th1 cell dynamics, incorporating differentiation via MDCs ($k_{20a}$ term) and both infected and activated macrophages acting as antigen presenting cells ($k_{29a}$ term), TNF-induced apoptosis ($k_{22a}$ term), and migration to the blood ($\xi_{1a}$ term).Equation (16) models naïve CD8+ T cell dynamics, and is similar to the naïve CD4+ cell equation (13). There is a source term ($s_{N8}$), and mechanisms for recruitment by MDCs ($k_{16}$ term), natural death, and differentiation to T80 cells ($k_{17}$ term). The $k_{17}$ term captures the role of licensed DCs in priming CD8+ T cells. Licensing is achieved by an initial successful CD4+ T cell priming: that is why CD8+ T cell priming is only possible if either precursor or fully effector Th1 cells are present. Equation (17) describes primed CD8+ T cell dynamics, with mechanisms for CD8+ T cell proliferation ($k_{18}$ term), differentiation and migration into the blood ($\xi_2$ term), similarly to equation (14).

Equations (18) and (19) describe IFN-γ-producing T8 cell and CTL dynamics in the lymph node (see [5]). Both equations capture differentiation induced by MDCs ($k_{24a}$ term) and by macrophages ($k_{30a}$ term), TNF-induced apoptosis ($k_{26a}$ and $k_{28a}$ terms), and migration to the blood ($\xi_{2a}$ and $\xi_{2b}$ terms). Parameter m allows for an overlap between IFN-γ-producing CD8+ T cell and CTLs.

*Naïve CD4+ T cells* - $(N_4)$

Source term; Extra recruitment (induced by MDC); Death and re-circulation; Naïve CD4+ T-cell differentiation to precursor Th1

$$\frac{dN_4}{dt} = s_{N_4} + k_{13} N_4 \left( \frac{MDC}{MDC + hs_{13}} \right) - \mu_{N_4} N_4 - k_{14}\ N_4\ MDC \tag{13}$$

*Precursor Th1 in the LN* $\left(\hat{T}_1^{LN}\right)$

Naïve CD4+ T cells differentiation to precursor Th1; Precursor Th1 cells net-proliferation (downregulated by IL10); Precursor Th1 cell migration into the BLOOD

$$\frac{d\hat{T}_1^{LN}}{dt} = k_{14}\ N_4\ MDC + k_{15}\hat{T}_1^{LN}\left(1 - \frac{\hat{T}_1^{LN}}{\delta_2}\right)\left(1 - \frac{I_{10}^{LN}}{I_{10}^{LN} + hs_{I_{10} - \hat{T}_1^{LN}}}\right) - \xi_1 \hat{T}_1^{LN} -$$

$$- k_{20a} I_{12}^{LN} \hat{T}_1^{LN} \left( \frac{MDC}{MDC + f_2 I_{10}^{LN} + hs_{20a}} \right) - \tag{14}$$

Th1 differentiation in the LN (induced by IL12 and MDC in the LN, downregulated by IL10)

$$- k_{29a} I_{12}^{LN} \hat{T}_1^{LN} \left( \frac{M_A^{LN} + w_1 M_I^{LN}}{M_A^{LN} + w_1 M_I^{LN} + hs_{29a}} \right)$$

INDEPENDENT Th1 differentiation in the LN (induced by IL12 and MA and MI presentation in the LN)

*Th1 in the LN* $\left(T_1^{LN}\right)$

Th1 differentiation in the LN (induced by IL12 and MDC in the LN, downregulated by IL10)

$$\frac{dT_1^{LN}}{dt} = k_{20a} I_{12}^{LN} \hat{T}_1^{LN} \left( \frac{MDC}{MDC + f_2 I_{10}^{LN} + hs_{20a}} \right) + k_{29a} I_{12}^{LN} \hat{T}_1^{LN} \left( \frac{M_A^{LN} + w_1 M_I^{LN}}{M_A^{LN} + w_1 M_I^{LN} + hs_{29a}} \right) -$$

$$- k_{22a} \left( \frac{F_\alpha^{LN}}{F_\alpha^{LN} + hs_{22a}} \right) T_1^{LN} - \xi_{1a} T_1^{LN} \tag{15}$$

TNF-induced apoptosis of Th1 in the LN

NET Th1 cell migration into the BLOOD: it discounts death and restimulation by MA and MI

*Naïve CD8+ T cells - $(N_8)$*

Source term; Recirculation and recruitment (by MDC); Death and re-circulation; Naïve CD8+ T-cell differentiation to T80

$$\frac{dN_8}{dt} = s_{N_8} + k_{16} N_8 \left( \frac{MDC}{MDC + hs_{16}} \right) - \mu_{N_8} N_8 - k_{17} N_8 MDC \left( \frac{\left[ T_1^{LN} + w_{T_{80}^{LN}} \hat{T}_1^{LN} \right]}{\left[ T_1^{LN} + w_{T_{80}^{LN}} \hat{T}_1^{LN} \right] + hs_{17}} \right) \quad (16)$$

*T80 in the LN $\left(T_{80}^{LN}\right)$*

Naïve CD8+ T cells differentiation to T80; T80 cells net-proliferation (downregulated by IL10); T80 migration into the BLOOD

$$\frac{dT_{80}^{LN}}{dt} = k_{17} N_8 MDC \left( \frac{\left[ T_1^{LN} + w_{T_{80}^{LN}} \hat{T}_1^{LN} \right]}{\left[ T_1^{LN} + w_{T_{80}^{LN}} \hat{T}_1^{LN} \right] + hs_{17}} \right) + k_{18} T_{80}^{LN} \left( 1 - \frac{T_{80}^{LN}}{\rho_3} \right) \left( 1 - \frac{I_{10}^{LN}}{I_{10}^{LN} + hs_{I_{10} - T_{80}^{LN}}} \right) - \xi_2 T_{80}^{LN} - \left( k_{24a} I_{12}^{LN} T_{80}^{LN} \left( \frac{MDC}{MDC + f_2 I_{10}^{LN} + hs_{24a}} \right) + k_{30a} I_{12}^{LN} T_{80}^{LN} \left( \frac{M_A^{LN} + w_1 M_I^{LN}}{M_A^{LN} + w_1 M_I^{LN} + hs_{30a}} \right) \right) \quad (17)$$

T80 differentiation to CTL ($T_C$) or $T_8$ in the LN (induced by IL-12 and MDC, downregulated by IL10)

INDEPENDENT T80 differentiation to CTL ($T_C$) or $T_8$ in the LN (induced by IL12 and MA and MI presentation)

*T8 in the LN $\left(T_8^{LN}\right)$*

$$\frac{dT_8^{LN}}{dt} = m \left( k_{24a} I_{12}^{LN} T_{80}^{LN} \left( \frac{MDC}{MDC + f_2 I_{10}^{LN} + hs_{24a}} \right) + k_{30a} I_{12}^{LN} T_{80}^{LN} \left( \frac{M_A^{LN} + w_1 M_I^{LN}}{M_A^{LN} + w_1 M_I^{LN} + hs_{30a}} \right) \right) - k_{26a} T_8^{LN} \left( \frac{F_\alpha^{LN}}{F_\alpha^{LN} + hs_{26a}} \right) - \xi_{2a} T_8^{LN} \quad (18)$$

TNF induced apoptosis of T8 in the LN

NET T8 cell migration into the BLOOD: it discounts death and restimulation by MA and MI

INDEPENDENT T80 differentiation to CTL ($T_C$) or $T_8$ in the LN (induced by IL12 and MA and MI presentation)

T80 differentiation to CTL ($T_C$) or $T_8$ in the LN (induced by IL-12 and MDC, downregulated by IL10)

*CTL in the LN $\left(T_C^{LN}\right)$*

$$\frac{dT_C^{LN}}{dt} = m \left( k_{24a} I_{12}^{LN} T_{80}^{LN} \left( \frac{MDC}{MDC + f_2 I_{10}^{LN} + hs_{24a}} \right) + k_{30a} I_{12}^{LN} T_{80}^{LN} \left( \frac{M_A^{LN} + w_1 M_I^{LN}}{M_A^{LN} + w_1 M_I^{LN} + hs_{30a}} \right) \right) - k_{28a} T_C^{LN} \left( \frac{F_\alpha^{LN}}{F_\alpha^{LN} + hs_{28a}} \right) - \xi_{2b} T_C^{LN} \quad (19)$$

TNF induced apoptosis of CTL in the LN

NET T8 cell migration into the BLOOD: it discounts death and restimulation by MA and MI

### *1.5. Lymphocytes Dynamics in the Lung*

We also modeled lymphocyte dynamics in the lung (see diagrams in Figures S4 and S5, CD4+ and CD8+ lymphocyte dynamics, respectively). Equation (20) describes the precursor Th1 cell dynamics. It accounts for several mechanisms: TNF-independent ($rc_5$ term) and TNF-dependent ($rc_6$) recruitment, proliferation (logistic with rate constant $k_{19}$, with IL10 down-regulation), differentiation to Th1 cells via MDCs ($k_{20}$ term), and differentiation to Th1 cells via activated and infected macrophages ($k_{29}$ term), both representing gain terms for equation (21), where we model Th1 cell dynamics in the lung. Recruitment ($rc_{5a}$ and $rc_{6a}$ terms) and apoptosis ($k_{22}$ term) mechanisms are described in equation (21), similarly to Th1 cell dynamics in the lymph node (equation (15)). Equation (22) describes precursor activated $T_8$ cell dynamics (T80) in the lung. The incorporated mechanisms are very similar to those in equations (20) and (21): TNF-independent ($rc_7$ term) and TNF-dependent recruitment ($rc_8$ term), proliferation (logistic with rate constant $k_{23}$, with IL10 down-regulation), differentiation to CTL due to MDCs ($k_{24}$ term), differentiation due to activated and infected macrophages ($k_{30}$ term), and natural death. Equation (23) describes IFN-γ producing CD8+ T cells. The dynamics are regulated by the following mechanisms: TNF-independent ($rc_{7a}$ term) and TNF-dependent ($rc_{8a}$ term) recruitment, differentiation from precursor activated CD8+ T cells ($k_{24}$ and $k_{30}$ terms), TNF-induced apoptosis ($k_{26}$ term), and natural death. Equation (24) models the CTLs, with similar mechanisms.

*Precursor Th1 in the Lung - $\left(\hat{T}_1\right)$*

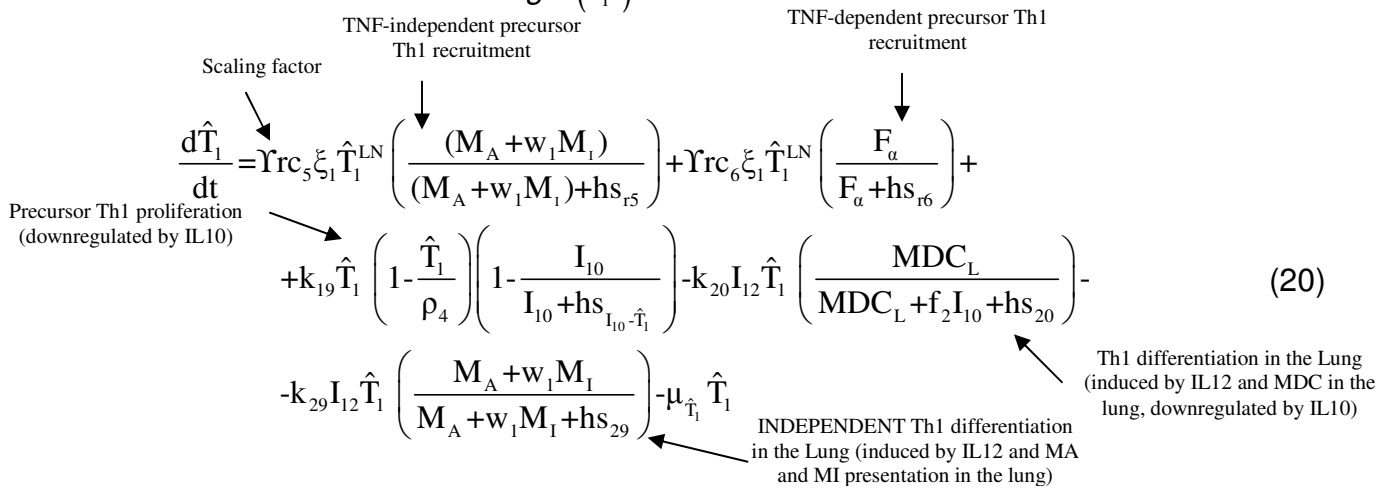


$$\frac{d\hat{T}_1}{dt}=\Upsilon rc_5\xi_1\hat{T}_1^{LN}\left(\frac{(M_A+w_1M_1)}{(M_A+w_1M_1)+hs_{r5}}\right)+\Upsilon rc_6\xi_1\hat{T}_1^{LN}\left(\frac{F_\alpha}{F_\alpha+hs_{r6}}\right)+$$
$$+k_{19}\hat{T}_1\left(1-\frac{\hat{T}_1}{\rho_4}\right)\left(1-\frac{I_{10}}{I_{10}+hs_{I_{10}-\hat{T}_1}}\right)-k_{20}I_{12}\hat{T}_1\left(\frac{MDC_L}{MDC_L+f_2I_{10}+hs_{20}}\right)- \quad (20)$$
$$-k_{29}I_{12}\hat{T}_1\left(\frac{M_A+w_1M_I}{M_A+w_1M_I+hs_{29}}\right)-\mu_{\hat{T}_1}\hat{T}_1$$

*T Helper 1 (Th1) in the Lung - $\left(T_1\right)$*

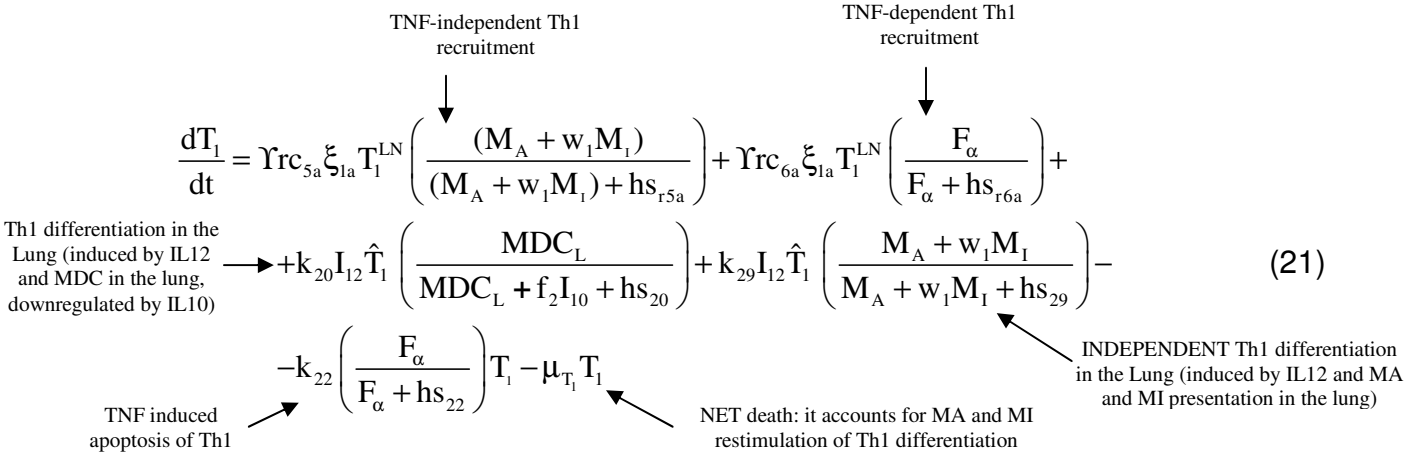


$$\frac{dT_1}{dt}=\Upsilon rc_{5a}\xi_{1a}T_1^{LN}\left(\frac{(M_A+w_1M_1)}{(M_A+w_1M_1)+hs_{r5a}}\right)+\Upsilon rc_{6a}\xi_{1a}T_1^{LN}\left(\frac{F_\alpha}{F_\alpha+hs_{r6a}}\right)+$$
$$+k_{20}I_{12}\hat{T}_1\left(\frac{MDC_L}{MDC_L+f_2I_{10}+hs_{20}}\right)+k_{29}I_{12}\hat{T}_1\left(\frac{M_A+w_1M_I}{M_A+w_1M_I+hs_{29}}\right)- \quad (21)$$
$$-k_{22}\left(\frac{F_\alpha}{F_\alpha+hs_{22}}\right)T_1-\mu_{T_1}T_1$$

*Precursor activated CD8+ T cells in the Lung - $\left(T_{80}\right)$*

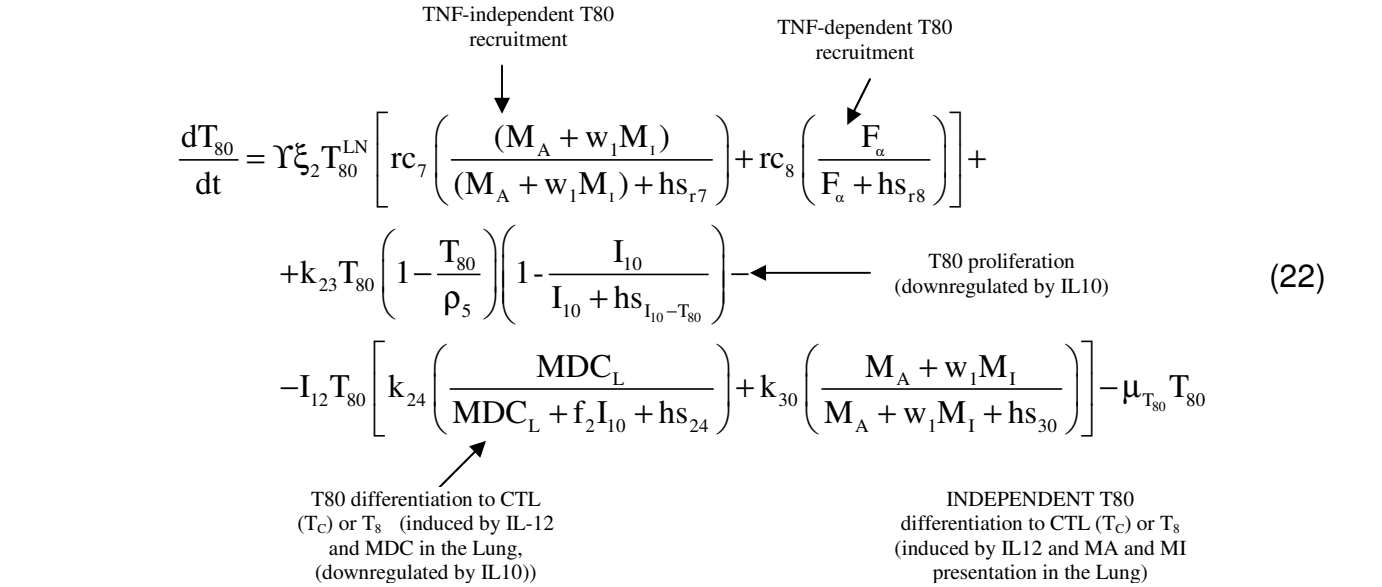


$$\frac{dT_{80}}{dt}=\Upsilon\xi_2T_{80}^{LN}\left[rc_7\left(\frac{(M_A+w_1M_1)}{(M_A+w_1M_1)+hs_{r7}}\right)+rc_8\left(\frac{F_\alpha}{F_\alpha+hs_{r8}}\right)\right]+$$
$$+k_{23}T_{80}\left(1-\frac{T_{80}}{\rho_5}\right)\left(1-\frac{I_{10}}{I_{10}+hs_{I_{10}-T_{80}}}\right)- \quad (22)$$
$$-I_{12}T_{80}\left[k_{24}\left(\frac{MDC_L}{MDC_L+f_2I_{10}+hs_{24}}\right)+k_{30}\left(\frac{M_A+w_1M_I}{M_A+w_1M_I+hs_{30}}\right)\right]-\mu_{T_{80}}T_{80}$$

*Subclass of activated CD8+ T cells in the Lung - $(T_8)$ (IFNγ-producing) CD8+ T cells*

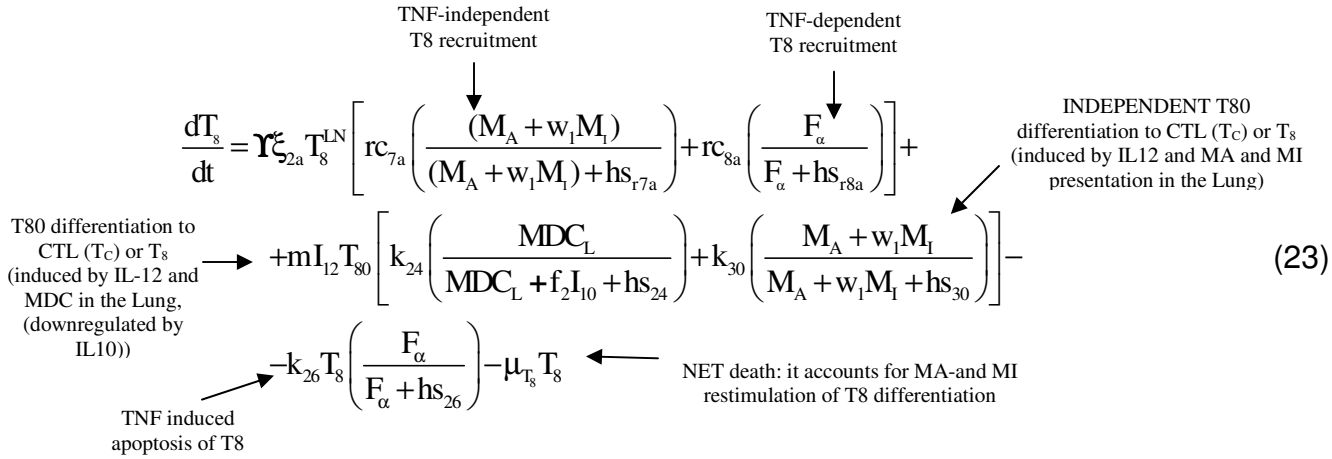


$$\frac{dT_8}{dt} = \Upsilon\xi_{2a} T_8^{LN}\left[rc_{7a}\left(\frac{(M_A + w_1 M_I)}{(M_A + w_1 M_I) + hs_{r7a}}\right) + rc_{8a}\left(\frac{F_\alpha}{F_\alpha + hs_{r8a}}\right)\right] + mI_{12}T_{80}\left[k_{24}\left(\frac{MDC_L}{MDC_L + f_2 I_{10} + hs_{24}}\right) + k_{30}\left(\frac{M_A + w_1 M_I}{M_A + w_1 M_I + hs_{30}}\right)\right] - k_{26}T_8\left(\frac{F_\alpha}{F_\alpha + hs_{26}}\right) - \mu_{T_8}T_8 \quad (23)$$

*Subclass of activated CD8+ T cells in the Lung (CTL) - $(T_C)$*

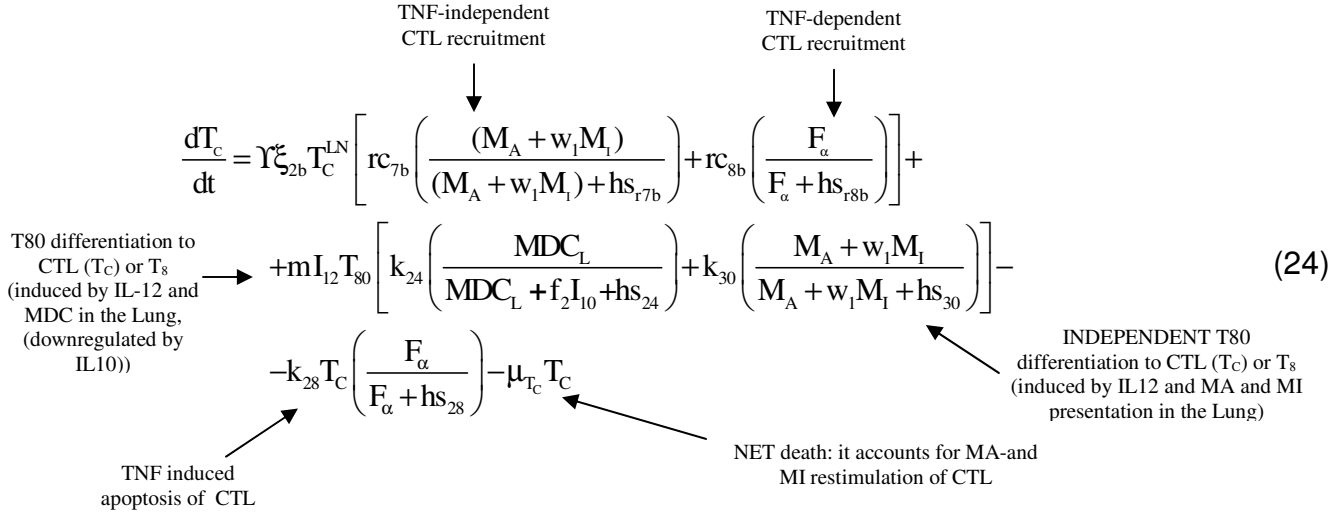


$$\frac{dT_C}{dt} = \Upsilon\xi_{2b} T_C^{LN}\left[rc_{7b}\left(\frac{(M_A + w_1 M_I)}{(M_A + w_1 M_I) + hs_{r7b}}\right) + rc_{8b}\left(\frac{F_\alpha}{F_\alpha + hs_{r8b}}\right)\right] + mI_{12}T_{80}\left[k_{24}\left(\frac{MDC_L}{MDC_L + f_2 I_{10} + hs_{24}}\right) + k_{30}\left(\frac{M_A + w_1 M_I}{M_A + w_1 M_I + hs_{30}}\right)\right] - k_{28}T_C\left(\frac{F_\alpha}{F_\alpha + hs_{28}}\right) - \mu_{T_C}T_C \quad (24)$$

### *1.6. Cytokine equations*

A table of cytokine dynamics is shown in Table S1, while the equations are described below. Cytokines are produced by a large variety of cells involved both in the innate and adaptive immunity [6]. We modeled four cytokines in both compartments: TNF-α, IFN-γ, IL-12 and IL-10. Table S1 lists cytokine production by cell types. Equations (25)-(28) describe cytokine dynamics in the lung, while equations (29)-(32) capture the dynamics in the LN. The equations for the same

cytokine are identical regardless the compartment, except for different values for the rates and rate constants. Each equation has a degradation rate for each cytokine represented by a $\mu$ coefficient. TNF$\alpha$ ($F_\alpha$, equation (25) and (29)) is mainly secreted by classically activated ($M_A$, $\alpha_1$ term) and infected ($M_I$, $\alpha_2$ term) macrophages, as well by mature DC (MDC, $\alpha_{16}$ term). The presence of bacteria (CFUlung) enhances TNF production by $M_A$, while IL-10 inhibits it. Lymphocytes also secrete TNF ($\alpha_3$ and $\alpha_4$) with similar regulatory mechanisms in place: classically activated macrophages ($M_A$) sustain TNF production, while IL-10 inhibits it.

IFN-$\gamma$ (equation (26) and (30)) is mainly secreted by lymphocytes (Th1 and IFN-$\gamma$-producing CD8+ Ts, $\alpha_5$ and $\alpha_6$ terms) in close interaction with classically activated macrophages [7,8]. Precursor Th1 and precursor effector CD8 Ts also secrete IFN-$\gamma$ ($\alpha_8$ and $\alpha_9$ terms), with the necessary stimulation of mature DC. Extra sources of IFN-$\gamma$ (e.g., natural killer cells - NKs) are active only if both bacteria and IL-12 are present ($s_g$ term). Infected macrophages produce a small amount of IFN-$\gamma$ ($\alpha_7$ terms).

IL-12 (equation (27) and (31)) is mainly produced by mature DC ($\alpha_{10}$) [9] and classically activated macrophages ($\alpha_{11}$) [10,11]: IFN-$\gamma$ increases IL-12 secretion, while IL-10 inhibits it [12]. IL-10 is produced by infected alternatively activated macrophages ($\alpha_{17}$) (equation (28) and (32)) [13]. Classically activated macrophages also participate in IL-10 production, either directly ($\alpha_{12}$) or enhancing effector T cell production ($\alpha_{14}$ and $\alpha_{15}$) [14]. Mature DC secrete some IL-10 as well ($\alpha_{13}$ term).

### *1.7. Cytokine production dynamics in the Lung*

*Tumor Necrosis Factor$\alpha$ –TNF$\alpha$ ($F_\alpha$,)*

$$\frac{dF_\alpha}{dt} = \alpha_1 M_A \left(1 + \frac{CFUlung}{CFUlung + f_3 I_{10} + chs_1}\right) + \alpha_2 M_I + \alpha_{16} MDC_L - \mu_{F_\alpha} F_\alpha + \\ + \left(\alpha_3 \left(\hat{T}_1 + T_1\right)\left(1 - \frac{I_{10}}{I_{10} + hs_{I_{10}-F_\alpha}}\right) + \alpha_4 \left(T_C + T_8 + T_{80}\right)\right)\left(1 + \frac{M_A}{M_A + chs_2}\right) \quad (25)$$

*Interferon $\gamma$ - IFN$\gamma$ ($I_\gamma$)*

$$\frac{dI_\gamma}{dt} = s_g \left(\frac{CFUlung}{CFUlung + chs_3}\right)\left(\frac{I_{12}}{I_{12} + chs_4}\right) + \alpha_5 T_1 \left(\frac{M_{ATot}}{M_{ATot} + f_2 I_{10} + chs_5}\right) + \\ + \alpha_6 T_8 \left(\frac{M_A}{M_A + chs_6}\right) + \alpha_7 M_I + \alpha_8 \hat{T}_1 \left(\frac{MDC_L}{MDC_L + f_2 I_{10} + chs_8}\right) + \quad (26) \\ + \alpha_9 T_{80} \left(\frac{MDC_L}{MDC_L + f_2 I_{10} + chs_9}\right) - \mu_{I_\gamma} I_\gamma$$

*Interlukin 12 – IL12 ($I_{12}$)*

$$\frac{dI_{12}}{dt} = \alpha_{10} MDC_L \left(1 + \frac{I_\gamma}{I_\gamma + f_4 I_{10} + chs_{10}}\right) - \mu_{I_{12}} I_{12} + \alpha_{11} M_A \left(1 + \frac{I_\gamma}{I_\gamma + f_4 I_{10} + chs_{11}}\right) \quad (27)$$

*Interlukin 10 – IL10 ($I_{10}$)*

$$\frac{dI_{10}}{dt} = \alpha_{17} M_I + \alpha_{12} M_A + \alpha_{13} MDC_L + \left(\alpha_{14} T_1 + \alpha_{15} (T_8 + T_C)\right)\left(1 + \frac{M_A}{M_A + chs_{15}}\right) - \mu_{I_{10}} I_{10} \quad (28)$$

### *1.8. Cytokine production dynamics in the Lymph Node*

*Tumor Necrosis Factor$\alpha$ –TNF$\alpha$ ($F_\alpha$,)*

$$\frac{dF_\alpha^{LN}}{dt} = \alpha_{1a} M_A^{LN} \left(1 + \frac{CFU\ln}{CFU\ln + f_3 I_{10}^{LN} + chs_{1a}}\right) + \alpha_{2a} M_I^{LN} + \alpha_{16a} MDC - \mu_{F_\alpha} F_\alpha^{LN} + \\ + \left(\alpha_{3a} \left(\hat{T}_1^{LN} + T_1^{LN}\right)\left(1 - \frac{I_{10}^{LN}}{I_{10}^{LN} + hs_{I_{10a}-F_\alpha}}\right) + \alpha_{4a} \left(T_C^{LN} + T_8^{LN} + T_{80}^{LN}\right)\right)\left(1 + \frac{M_A^{LN}}{M_A^{LN} + chs_{2a}}\right) \quad (29)$$

*Interferon γ - IFNγ ($I_\gamma$)*

$$\frac{dI_\gamma^{LN}}{dt} = s_g^{LN}\left(\frac{CFU\ln}{CFU\ln + chs_{3a}}\right)\left(\frac{I_{12}^{LN}}{I_{12}^{LN} + chs_{4a}}\right) + \alpha_{5a}T_1^{LN}\left(\frac{M_A^{LN}}{M_A^{LN} + chs_{5a}}\right) + \\ + \alpha_{6a}T_8^{LN}\left(\frac{M_A^{LN}}{M_A^{LN} + chs_{6a}}\right) + \alpha_{7a}M_I^{LN} + \alpha_{8a}\hat{T}_1^{LN}\left(\frac{MDC}{MDC + f_2 I_{10}^{LN} + chs_{8a}}\right) + \\ + \alpha_{9a}T_{80}^{LN}\left(\frac{MDC}{MDC + f_2 I_{10}^{LN} + chs_{9a}}\right) - \mu_g I_\gamma \qquad (30)$$

*Interlukin 12 – IL12 ($I_{12}$)*

$$\frac{dI_{12}^{LN}}{dt} = \alpha_{10a}MDC\left(1 + \frac{I_\gamma^{LN}}{I_\gamma^{LN} + f_4 I_{10}^{LN} + chs_{10a}}\right) + \alpha_{11a}M_A^{LN}\left(1 + \frac{I_\gamma^{LN}}{I_\gamma^{LN} + f_4 I_{10}^{LN} + chs_{11a}}\right) - \mu_{I_{12}} I_{12}^{LN} \qquad (31)$$

*Interlukin 10 – IL10 ($I_{10}$)*

$$\frac{dI_{10}^{LN}}{dt} = \alpha_{17a}M_I^{LN} + \alpha_{12a}M_A^{LN} + \alpha_{13a}MDC - \mu_{I_{10}} I_{10}^{LN} + \\ + \left(\alpha_{14a}T_1^{LN} + \alpha_{15a}(T_C^{LN} + T_8^{LN})\right)\left(1 + \frac{M_A^{LN}}{M_A^{LN} + chs_{15a}}\right) \qquad (32)$$

### *1.9. Comparing parameter estimates*

Based on the parameter estimation results, we compare several biological mechanisms across different cell types and different scales/compartments. Table S2 summarizes parameter estimation results (see Baseline (best fit) column). We find differences between TNF-independent recruitment parameters comparing monocyte derived cells (macrophages, $rc_1$ and DCs, $rc_3$) and lymphocytes ($rc_5$, $rc_7$), with the latter having 2 orders of magnitude lower maximum recruitment rates. Resting macrophages in the lung seem to have a higher estimated recruitment rates (5 times higher than any other monocyte derived cell types, both in the lung and lymph node compartment).

TNF-dependent recruitment parameter estimates ($rc_2$, $rc_4$) are consistently higher in the lung than in the lymph node for macrophages and DCs. Maximum recruitment rates for T cells ($rc_5$, $rc_6$, $rc_7$, $rc_8$) are always 3-4 orders of magnitude lower than macrophages and DCs ($rc_2$, $rc_4$). Precursor effector T cells are recruited to the lung with rates 1 to 2 orders of magnitude higher than fully effector CD4+ and CD8+ T cells, suggesting that most of the final T cell differentiation happens at the site of infection.

Estimated rates of bacteria uptake by macrophages ($k_1$) and DCs ($k_{12}$) are similar, as well the rates of macrophage activation ($k_2$, $k_7$). Given similar inflammation conditions (i.e., the function $\delta$), the estimates for $M_1$ (CAM) activation rates ($k_2$) are 5 times higher than $M_2$ ($k_7$, AAM). This suggests how a pro-inflammatory cytokine environment (IFN-$\gamma$ and TNF) acts synergistically towards a protective Th1 response (CAM).

Macrophage bursting, TNF and Fas/FasL induced apoptosis, as well as CTL killing of infected macrophages shared no significant differences in estimated maximum rates and half saturation constants. In the lymph node compartment, maximum recruitment rates of naïve CD4+ and CD8+ T cells induced by mature DCs are similar ($k_{13}$, $k_{16}$), as well as the priming rates ($k_{14}$, $k_{17}$) and precursor effector T cell proliferation ($k_{15}$, $k_{18}$). T cell TNF-induced apoptosis rates ($k_{22}$, $k_{26}$, $k_{28}$) are higher than T cell differentiation rates ($k_{20}$, $k_{29}$, $k_{24}$, $k_{30}$), and overall they are 1-2 orders of magnitude higher at the site of infection than in the lymph node ($k_{22a}$, $k_{26a}$, $k_{28a}$).

The estimate for the scaling parameter (scaling) is approximately set to 2, suggesting how cells migrating to the site of infection could come at most from one more lymph node source, which is consistent with the mouse anatomy. The estimated MDC migration rate $\varphi$ is 0.5, predicting that on average a DC will migrate out of the site of infection within 40 hours upon maturation.

# SUPPLEMENTARY FIGURES

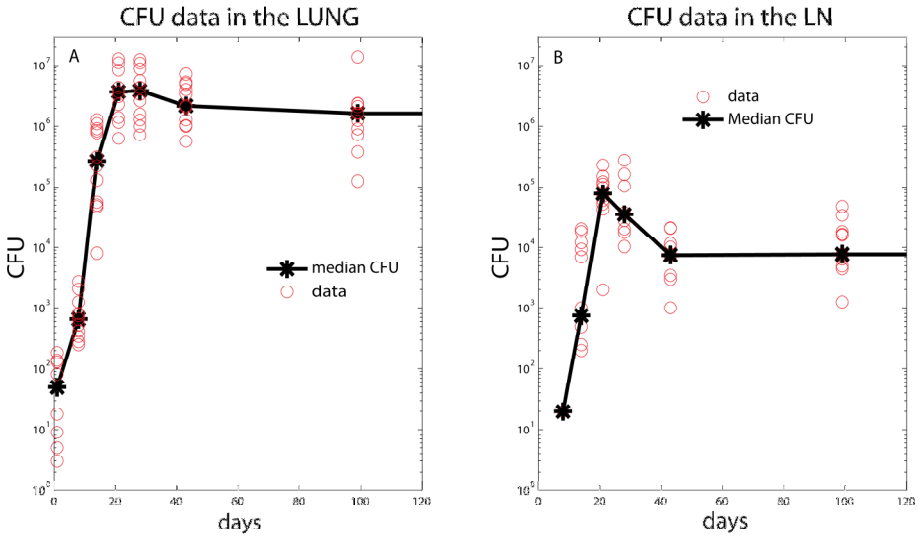


**Figure S1**: Experimental data (red circles) and median trajectory (black line with stars) for bacterial counts in the lung (Panel A) and lymph node (Panel B). Each point (red circle) represents a measure of bacterial load in the whole organ (either lung or lymph node) of a mouse. Mice were sacrificed at day 1, 8, 14, 21, 28, 43 and 99, for a total of 80 mice (12 mice per each time point, except for day 1 where only 8 mice were sacrificed).

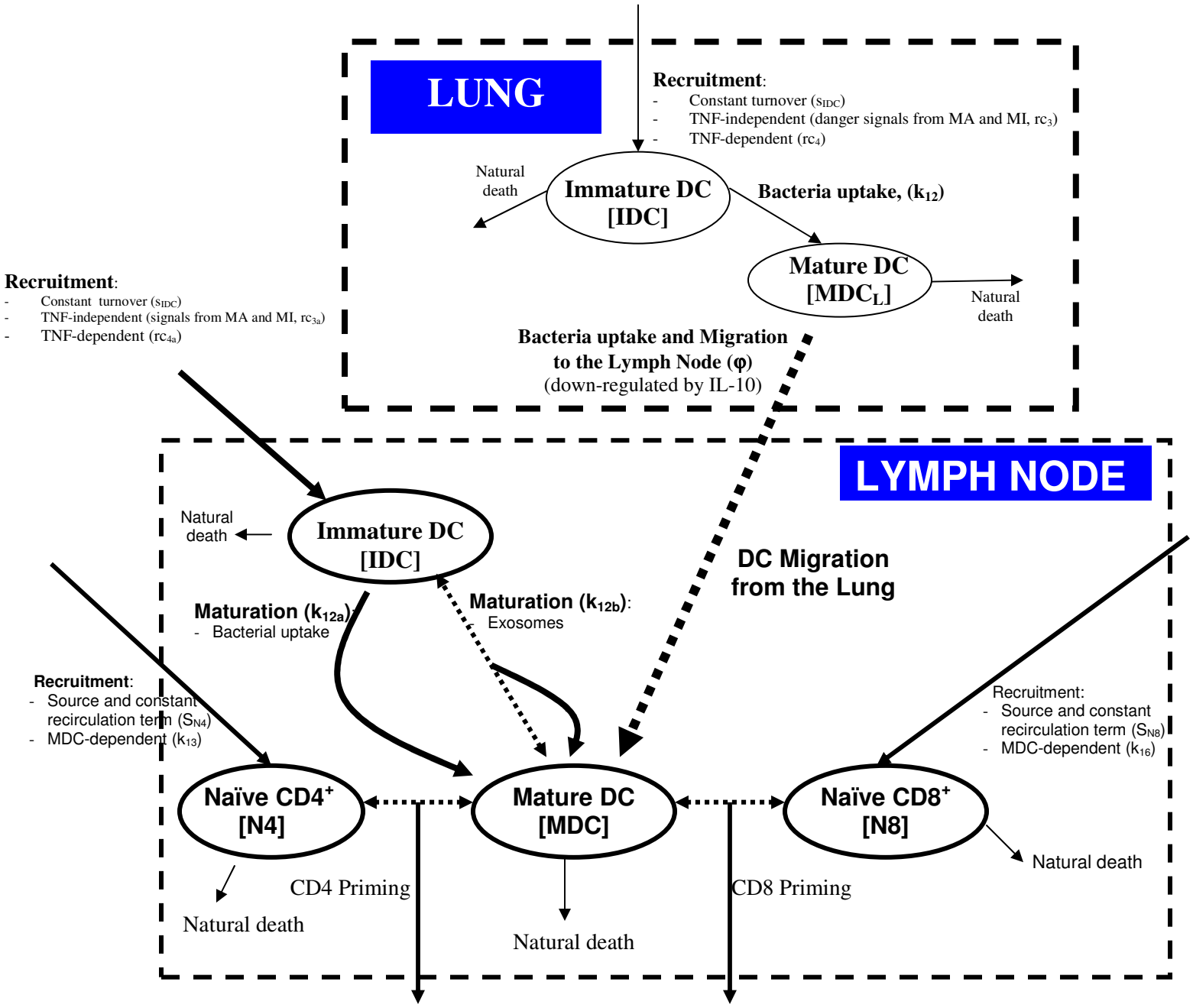


**Figure S2**: diagram of DC dynamics in the lung and in the lymph node that are represented in the model. The parameters in parenthesis represent how each mechanism is described in the model equations. CFU input/forcing functions affect the braches describing IDC maturation in both compartments.

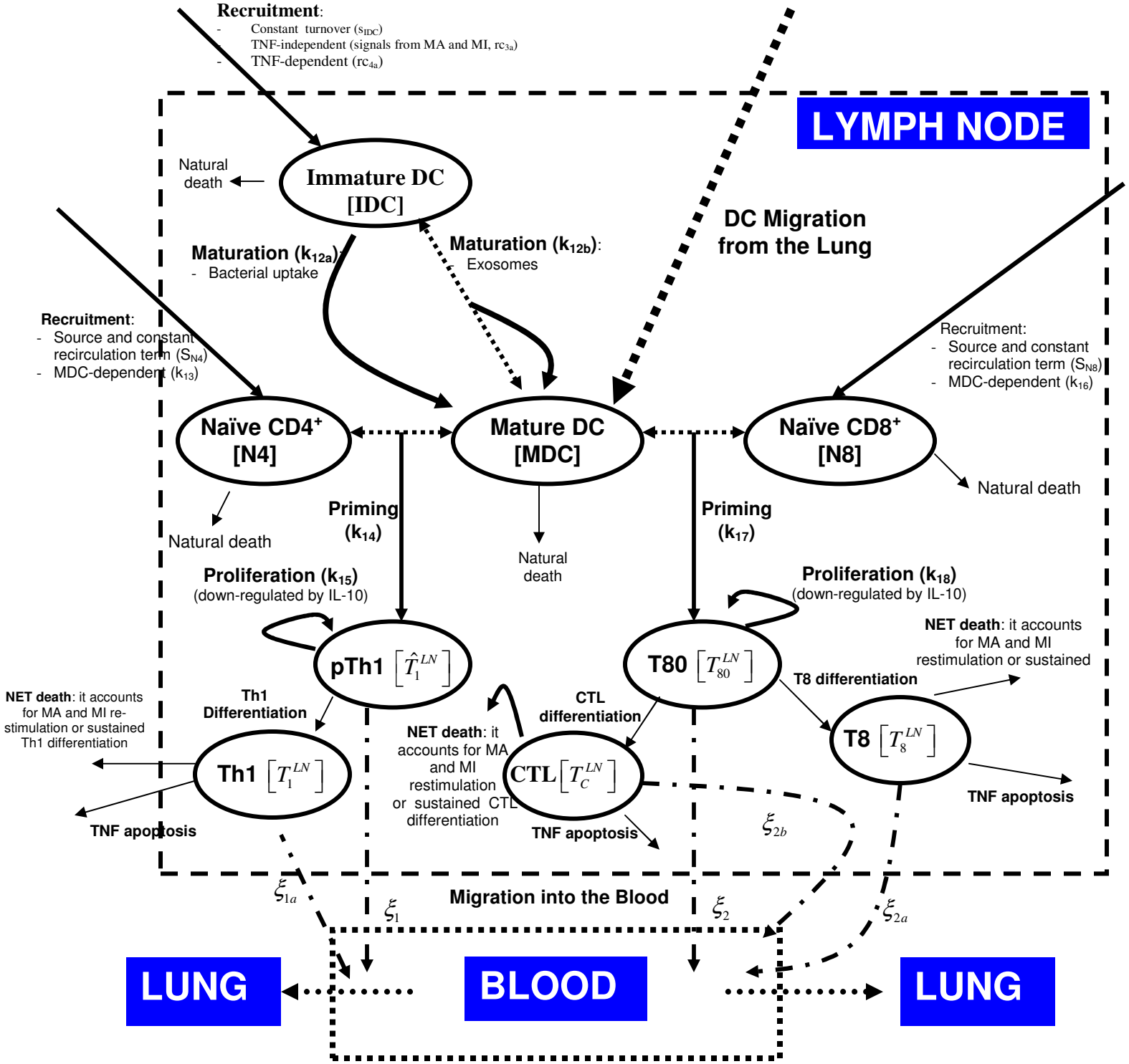


**Figure S3**: diagram of DCs and Lymphocytes dynamics in the lymph node that are represented in the model. The parameters in parenthesis represent how each mechanism is described in the model equations. CFU input/forcing function affects the brach describing IDC maturation.

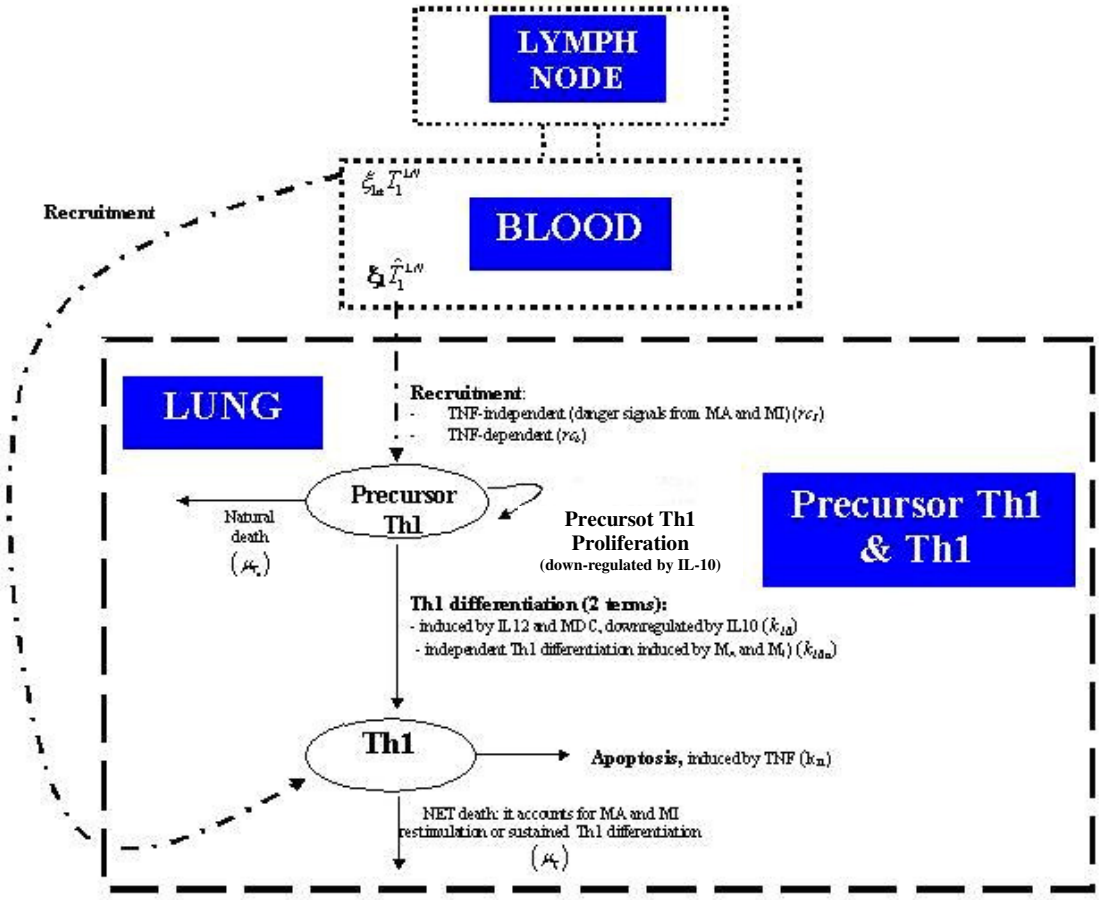


**Figure S4**: diagram of CD4+ Ts dynamics in the lung that are represented in the model. The parameters in parenthesis represent how each mechanism is described in the model equations.

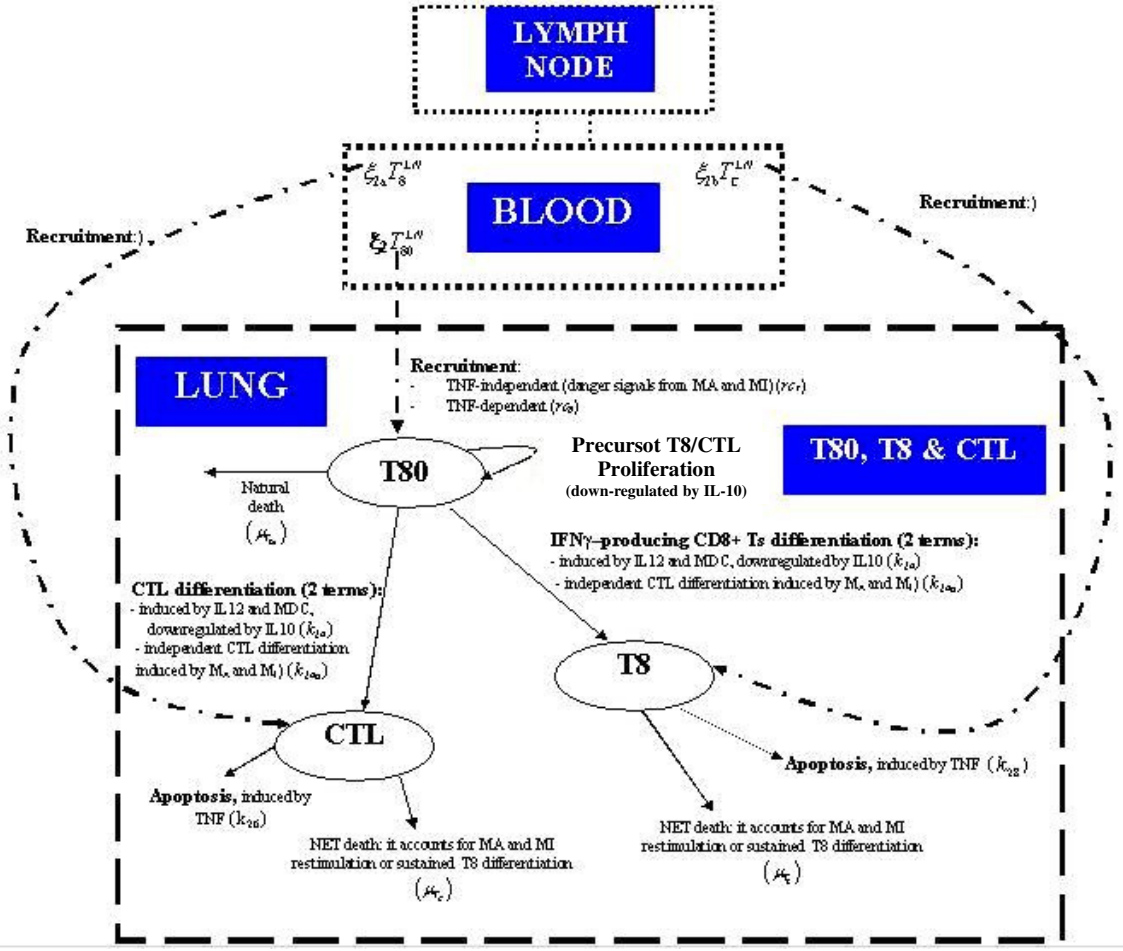


**Figure S5**: diagram of CD8+ Ts dynamics in the lymph node that are represented in the model. The parameters in parenthesis represent how each mechanism is described in the model equations.

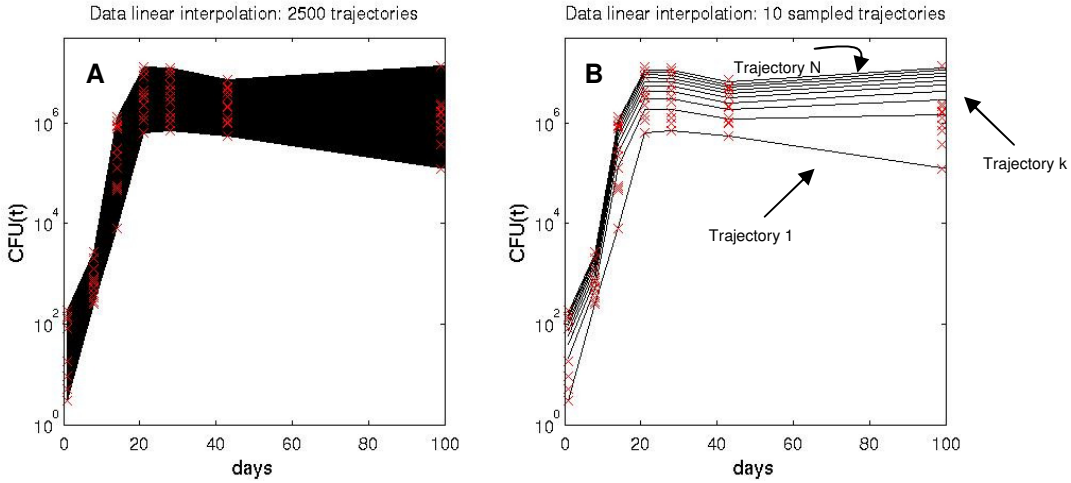


**Figure S6**: procedure to translate experimental data to a functional for virtual CFU trajectories. *Panel A*: LHS2 for CFU. The red x are the experimental data. The black lines are the result of stepwise linear interpolation of 2500 samples at each experimental time point. *Panel B*: subset of 2500 virtual CFU trajectories shown in Panel A. The minimum and the maximum values for the experimental data at each time point are connected and they define respectively trajectory 1 and trajectory N (N=2500) in LHS2.

# SUPPLEMENTARY TABLES

**Table S1**: cytokine production table. Cell types are listed as producers of the cytokines in the model. The order reflects the known or presumed relative importance of each cell in producing each cytokine. We assume that the order is the same for both compartments (lung and lymph node).

| Variable | Cells producing |
|---|---|
| TNFα [ $F_\alpha$ ] | 1) Activated Macs [ $M_A$ ] , Infected Macs [ $M_I$ ] , Mature [$MDC_L$]<br>2) Th1 [ $T_1$ ], IFN-γ producing CD8 [ $T_8$ ] , CTL [ $T_C$ ]<br>3) Precursor Th1 [ $\hat{T}_1$ ] , Precursor effector CD8 [ $T_{80}$ ] |
| IFNγ [ $I_\gamma$ ] | 1) Th1 [ $T_1$ ], IFN-γ producing CD8 [ $T_8$ ]<br>2) Infected Macs [ $M_I$ ]<br>3) Precursor Th1 [ $\hat{T}_1$ ] , Precursor effector CD8 [ $T_{80}$ ] |
| IL12 [ $I_{12}$ ] | 1) Mature [$MDC_L$]<br>2) Activated [ $M_A$ ] |
| IL10 [ $I_{10}$ ] | 1) Infected Macrophages (Infected M2 or AAM)<br>2) Activated [ $M_A$ ]<br>3) Mature [$MDC_L$]<br>4) Th1 [ $T_1$ ], IFN-γ producing CD8 [ $T_8$ ] , CTL [ $T_C$ ] |

**Table S2**: list of parameter names, descriptions, best fit values (from the model fitting algorithm) and the ranges used to screen the parameter space and select an adequate initial condition for the fitting algorithm.

| Name | Description | Baseline (best fit) | LHS1 ranges |
|---|---|---|---|
| *rc1* | max TNF-independent MR recruitment rate | 5.00E+03 | [1E-1,1E5] |
| *rc1a* | max TNF-independent MR recruitment rate (LN) | 5.00E+03 | [1E-1,1E5] |
| *rc3* | max TNF-independent IDC recruitment rate | 1.00E+03 | [1E-1,1E5] |
| *rc3a* | max TNF-independent IDC recruitment rate (LN) | 1.00E+02 | [1E-1,1E5] |
| *rc5* | max TNF-independent precursor Th1 recruitment rate (Lung) | 1.00E+01 | [1E-3,1E5] |
| *rc5a* | max TNF-independent Th1 recruitment rate (Lung) | 1.00E-01 | [1E-3,1E5] |
| *rc7* | max TNF-independent precursor T8/CTL recruitment rate (Lung) | 1.00E+01 | [1E-3,1E5] |
| *rc7a* | max TNF-independent T8 recruitment rate (Lung) | 5.00E-01 | [1E-3,1E5] |
| *rc7b* | max TNF-independent CTL recruitment rate (Lung) | 5.00E-01 | [1E-3,1E5] |
| *hsr1* | Half-sat for TNF-independent MR recruitment rate | 1.00E+03 | [1,1E6] |
| *hsr1a* | Half-sat for TNF-independent MR recruitment rate (LN) | 1.00E+02 | [1,1E6] |
| *hsr3* | Half-sat for TNF-independent IDC recruitment rate | 1.00E+04 | [1,1E6] |
| *hsr3a* | Half-sat for TNF-independent IDC recruitment rate (LN) | 1.00E+04 | [1,1E6] |
| *hsr5* | Half-sat for TNF-independent precursor Th1 recruitment rate (Lung) | 1.00E+02 | [1,1E6] |
| *hsr5a* | Half-sat for TNF-independent Th1 recruitment rate (Lung) | 1.00E+02 | [1,1E6] |
| *hsr7* | Half-sat for TNF-independent precursor T8/CTL recruitment rate (Lung) | 1.00E+02 | [1,1E6] |
| *hsr7a* | Half-sat for TNF-independent T8 recruitment rate (Lung) | 1.00E+02 | [1,1E6] |
| *hsr7b* | Half-sat for TNF-independent CTL recruitment rate (Lung) | 1.00E+02 | [1,1E6] |
| *rc2* | max TNF-dependent MR recruitment rate | 1.00E+04 | [1E-3,1E5] |
| *rc2a* | max TNF-dependent MR recruitment rate (LN) | 2.5E+03 | [1E-3,1E5] |
| *rc4* | max TNF-dependent IDC recruitment rate | 5.00E+03 | [1E-3,1E5] |
| *rc4a* | max TNF-dependent IDC recruitment rate (LN) | 1.00E+03 | [1E-3,1E5] |
| *rc6* | max TNF-dependent precursor Th1 recruitment rate (Lung) | 1 | [1E-3,1E5] |
| *rc6a* | max TNF-dependent Th1 recruitment rate (Lung) | 1.00E-01 | [1E-3,1E5] |
| *rc8* | max TNF-dependent precursor T8/CTL recruitment rate (Lung) | 1 | [1E-3,1E5] |
| *rc8a* | max TNF-dependent T8 recruitment rate (Lung) | 5.00E-01 | [1E-3,1E5] |
| *rc8b* | max TNF-dependent CTL recruitment rate (Lung) | 5.00E-01 | [1E-3,1E5] |
| *hsr2* | Half-sat for TNF-dependent MR recruitment rate | 1.00E+01 | [1E-3,1E3] |
| *hsr2a* | Half-sat for TNF-dependent MR recruitment rate (LN) | 107.5372 | [1E-3,1E3] |
| *hsr4* | Half-sat for TNF-dependent IDC recruitment rate | 1.00E+01 | [1E-3,1E3] |
| *hsr4a* | Half-sat for TNF-dependent IDC recruitment rate (LN) | 1 | [1E-3,1E3] |
| *hsr6* | Half-sat for TNF-dependent precursor Th1 recruitment rate (Lung) | 0.30464 | [1E-3,1E3] |
| *hsr6a* | Half-sat for TNF-dependent Th1 recruitment rate (Lung) | 0.48059 | [1E-3,1E3] |
| *hsr8* | Half-sat for TNF-dependent precursor T8/CTL recruitment rate (Lung) | 0.01 | [1E-3,1E3] |
| *hsr8a* | Half-sat for TNF-dependent T8 recruitment rate (Lung) | 0.57839 | [1E-3,1E3] |
| *hsr8b* | Half-sat for TNF-dependent CTL recruitment rate (Lung) | 0.2962 | [1E-3,1E3] |
| *k1* | M2 infection rate (Lung) | 1.00E-05 | [1E-8,1E2] |
| *k1a* | AAM infection rate (LN) | 3.00E-06 | [1E-8,1E2] |
| *k2* | MR classical activation rate (Lung) | 5.00E-01 | [1E-8,1E2] |
| *k2a* | MR classical activation rate (LN) | 5.00E-01 | [1E-8,1E2] |
| *k7* | MR alternative activation rate (Lung) | 1.00E-01 | [1E-8,1E2] |
| *k7a* | MR alternative activation rate (LN) | 1.00E-01 | [1E-8,1E2] |
| *k21* | M2 classical activation rate (Lung) | 1.00E-04 | [1E-8,1E2] |
| *k21a* | M2 classical activation rate (LN) | 1.00E-04 | [1E-8,1E2] |
| *hs2* | Half-sat of IFN in macrophage activation (Lung) | 1 | [1E-3,1E2] |
| *hs3* | Half-sat of Bacteria+TNF in macrophage activation (Lung) | 1.00E+03 | [1E1,1E8] |
| *hs2a* | Half-sat of IFN in macrophage activation (LN) | 1 | [1E-3,1E2] |
| *hs3a* | Half-sat of Bacteria+TNF in macrophage activation (LN) | 1.00E+05 | [1E1,1E8] |
| *k3* | MI maximum bursting rate (Lung) | 1.00E-01 | [1E-8,1E2] |
| *k3a* | MI maximum bursting rate (LN) | 1.00E-01 | [1E-8,1E2] |
| *k4* | MI maximum Fas/FasL-apoptosis rate (Lung) | 1.00E-01 | [1E-8,1E2] |
| *k4a* | MI maximum Fas/FasL-apoptosis rate (LN) | 1.00E-01 | [1E-8,1E2] |
| *hs4* | Th1 half-sat on MI Fas/FasL-apoptosis rate (Lung) | 1241.132 | [1,1E5] |
| *hs4a* | Th1 half-sat on MI Fas/FasL-apoptosis rate (LN) | 1262.4551 | [1,1E5] |
| *k5* | MI maximum TNF-apoptosis rate (Lung) | 1.00E-01 | [1E-8,1E2] |

| | | | |
|---|---|---|---|
| *k5a* | MI maximum TNF-apoptosis rate (LN) | 1.00E-01 | [1E-8,1E2] |
| *hs5* | TNF half-sat on MI TNF-apoptosis rate (Lung) | 0.19312 | [1E-3,1E1] |
| *hs5a* | TNF half-sat on MI TNF-apoptosis rate (LN) | 0.2 | [1E-3,1E1] |
| *k6* | MI maximum CTL killing rate (Lung) | 1.00E-01 | [1E-8,1E2] |
| *k6a* | MI maximum CTL killing rate (LN) | 1.00E-01 | [1E-8,1E2] |
| *hs6* | CTL half-sat onMI CTL killing rate (Lung) | 88.0301 | [1,1E5] |
| *hs6a* | CTL half-sat on MI CTL killing rate (LN) | 88 | [1,1E5] |
| *hsI10* | IL10 half saturation on delaying macrophage activation (Lung) | 1 | [1E-3,1E4] |
| *hsI10a* | IL10 half saturation on delaying macrophage activation (LN) | 1 | [1E-3,1E4] |
| *hsI10_DC* | IL10 half saturation on delaying IDC maturation (Lung) | 1 | [1E-3,1E4] |
| *hsI10_DCLN* | IL10 half saturation on delaying IDC maturation (LN) | 1.00E+03 | [1E-3,1E4] |
| *hsI10_T0* | IL10 half saturation on delaying precursor Th1 proliferation (Lung) | 1 | [1E-3,1E4] |
| *hsI10_T0LN* | IL10 half saturation on delaying precursor Th1 proliferation (LN) | 1 | [1E-3,1E4] |
| *hsI10_T80* | IL10 half saturation on delaying precursor T8/CTL proliferation (Lung) | 1 | [1E-3,1E4] |
| *hsI10_T80LN* | IL10 half saturation on delaying precursor T8/CTL proliferation (LN) | 1 | [1E-3,1E4] |
| *hsI10_TNF* | IL10 half saturation on delaying TNF production by precursor and effector Th1 (Lung) | 1 | [1E-3,1E4] |
| *hsI10a_TNF* | IL10 half saturation on delaying TNF production by precursor and effector Th1 (Lung) | 1 | [1E-3,1E4] |
| *k12* | IDC infection rate (Lung) | 1.00E-06 | [1E-8,1E2] |
| *k12a* | IDC infection rate (LN) | 1.00E-08 | [1E-8,1E2] |
| *k12b* | IDC maximum bacteria uptake rate [exosome] (LN) | 1.00E-08 | [1E-8,1E2] |
| *hs12b* | MDC half-sat on IDC bacteria uptake (LN) | 565.7622 | [1,1E4] |
| *k13* | Naïve CD4+ T cells maximum MDC-dependent recruitment rate (LN) | 7 | [1E-3,1E4] |
| *hs13* | MDC half-sat Naïve CD4+ T cells recruitment rate (LN) | 1.00E+03 | [1,1E4] |
| *k14* | Rate (likelyhood) of Naïve CD4+ T cell priming when encountering a MDC (LN) | 1.50E-03 | [1E-6,1] |
| *k15* | Precursor Th1 proliferation rate (LN) | 2 | [1E-3,1E4] |
| *rho2* | Precursor Th1 carrying capacity (LN) | 1.00E+07 | [1E4,1E8] |
| *k20a* | Maximum Th1 differentiation rate, dependent of IL12 and MDC (LN) | 1.00E-03 | [1E-6,1E1] |
| *hs20a* | MDC half-sat on IL12 and MDC dependent Th1 differentiation (LN) | 1.00E+03 | [1,1E4] |
| *k29a* | Maximum Th1 differentiation rate, dependent of IL12 and Macrophages (LN) | 1.00E-03 | [1E-6,1E1] |
| *hs29a* | MDC half-sat on IL12 and Macrophages dependent Th1 differentiation (LN) | 1.00E+03 | [1,1E4] |
| *k22a* | Maximum rate of TNF-dependent apoptosis of Th1 cells (LN) | 1.00E-01 | [1E-6,1E1] |
| *hs22a* | TNF half-sat for TNF-dependent apoptosis of Th1 cells (LN) | 1 | [1E-3,1E2] |
| *k16* | Naïve CD8+ T cells maximum MDC-dependent recruitment rate (LN) | 5 | [1E-3,1E4] |
| *hs16* | MDC half-sat Naïve CD8+ T cells recruitment rate (LN) | 1.00E+03 | [1,1E4] |
| *k17* | Maximum rate (likelyhood) of Naïve CD8+ T cell priming when encountering a MDC (LN) | 1.00E-03 | [1E-6,1] |
| *hs17* | Th1 half-sat rate for Naïve CD8+ T cell priming when encountering a MDC (LN) | 1.00E+01 | [1E-3,1E2] |
| *k18* | Precursor T8/CTL proliferation rate (LN) | 2 | [1E-3,1E4] |
| *rho3* | Precursor T8/CTL carrying capacity (LN) | 1.00E+07 | [1E4,1E8] |
| *k24a* | Maximum T8/CTL differentiation rate, dependent of IL-12 and MDC (LN) | 1.00E-04 | [1E-6,1E1] |
| *hs24a* | MDC half-sat on IL-12 and MDC dependent T8/CTL differentiation (LN) | 1.00E+03 | [1,1E4] |
| *k30a* | Maximum T8/CTL differentiation rate, dependent of IL-12 and Macrophages (LN) | 1.00E-04 | [1E-6,1E1] |
| *hs30a* | MDC half-sat on IL-12 and Macrophages dependent T8/CTL differentiation (LN) | 1.00E+03 | [1,1E4] |
| *k26a* | Maximum rate of TNF-dependent apoptosis of T8 cells (LN) | 1.00E-01 | [1E-6,1E1] |
| *hs26a* | TNF half-sat for TNF-dependent apoptosis of T8 cells (LN) | 1.00E-02 | [1E-3,1E2] |
| *k28a* | Maximum rate of TNF-dependent apoptosis of CTL cells (LN) | 1.00E-01 | [1E-6,1E1] |
| *hs28a* | TNF half-sat for TNF-dependent apoptosis of CTL cells (LN) | 1.00E-01 | [1E-3,1E2] |
| *csi1* | Precursor Th1 cells migration rate out of the LN into the blood | 5 | [1E-2,1E3] |
| *csi1a* | Th1 cells migration rate out of the LN into the blood | 1.00E+02 | [1E-2,1E3] |
| *csi2* | Precursor T8/CTL cells migration rate out of the LN into the blood | 1.00E+01 | [1E-2,1E3] |
| *csi2a* | T8 cells migration rate out of the LN into the blood | 1.00E+01 | [1E-2,1E3] |
| *csi2b* | CTL cells migration rate out of the LN into the blood | 1.00E+01 | [1E-2,1E3] |
| *k19* | Precursor Th1 proliferation rate (Lung) | 1.00E-01 | [1E-3,1E4] |
| *rho4* | Precursor Th1 carrying capacity (Lung) | 1.00E+05 | [1E4,1E8] |
| *k20* | Maximum Th1 differentiation rate, dependent of IL12 and MDC (Lung) | 1.00E-03 | [1E-6,1E1] |
| *hs20* | MDC half-sat on IL12 and MDC dependent Th1 differentiation (Lung) | 1.00E+03 | [1,1E4] |
| *k29* | Maximum Th1 differentiation rate, dependent of IL-12 and Macrophages (Lung) | 1.00E-03 | [1E-6,1E1] |
| *hs29* | MDC half-sat on IL-12 and Macrophages dependent Th1 differentiation (Lung) | 1.00E+03 | [1,1E4] |
| *k22* | Maximum rate of TNF-dependent apoptosis of Th1 cells (Lung) | 1.00E+01 | [1E-6,1E1] |
| *hs22* | TNF half-sat for TNF-dependent apoptosis of Th1 cells (Lung) | 1 | [1E-3,1E2] |
| *k23* | Precursor T8/CTL proliferation rate (Lung) | 1.00E-01 | [1E-3,1E4] |
| *rho5* | Precursor T8/CTL carrying capacity (Lung) | 1.00E+05 | [1E4,1E8] |
| *k24* | Maximum T8/CTL differentiation rate, dependent of IL-12 and MDC (Lung) | 1.00E-04 | [1E-6,1E1] |
| *hs24* | MDC half-sat on IL-12 and MDC dependent T8/CTL differentiation (Lung) | 27.6032 | [1,1E4] |
| *k30* | Maximum T8/CTL differentiation rate, dependent of IL-12 and Macrophages (Lung) | 1.00E-04 | [1E-6,1E1] |

| | | | |
|---|---|---|---|
| *hs30* | MDC half-sat on IL-12 and Macrophages dependent T8/CTL differentiation (Lung) | 166.9184 | [1,1E4] |
| *k26* | Maximum rate of TNF-dependent apoptosis of T8 cells (Lung) | 1 | [1E-6,1E1] |
| *hs26* | TNF half-sat for TNF-dependent apoptosis of T8 cells (Lung) | 1 | [1E-3,1E2] |
| *k28* | Maximum rate of TNF-dependent apoptosis of CTL cells (Lung) | 1 | [1E-6,1E1] |
| *hs28* | TNF half-sat for TNF-dependent apoptosis of CTL cells (Lung) | 1 | [1E-3,1E2] |
| *fi* | MDC migration rate from the lung to the LN | 0.75 | [1E-4,1] |
| *f1* | Scaling factor between TNF and CFU | 1.00E+02 | [1,1E5] |
| *f2* | Scaling factor between IL-10 and MDC | 0.12698 | [1E-2,1E2] |
| *f3* | Scaling factor between IL-10 and CFU | 4500.72 | [1,1E5] |
| *f4* | Scaling factor between IL-10 and IFN-g | 1.00E+01 | [1E-1,1E3] |
| *w1* | Weight factor between MA and MI | 1 | [1E-2,1E1] |
| *wT80* | Weight factor between precursor Th1 and Th1 in Naïve CD8 differentiation | 0.5 | [1E-2,1E1] |
| *scaling* | Scaling factor between lung and LN compartments | 2 | [1E-1,1E1] |
| *m* | Fraction of overlap between T8 (IFN producting CD8+ Ts) and CTL phenotypes | 0.75 | [1e-3,1] |

## HALF LIVES and CYTOKINES parameters (not included in the fitting)

| Name | Description | Baseline | LHS1 ranges) |
|---|---|---|---|
| $s_{M0}$ [$=(\mu_{M0}+k_7)*M_0(0)$] | Constant source of M0 (Lung) | 213.86 | none |
| $s_{M0}$ [$=(\mu_{M0}+k_{7a})*M_0^{LN}(0)$] | Constant source of M0 (LN) | 53.465 | none |
| $s_{IDC}$ [$=\mu_{IDC}*IDC(0)$] | Constant source of IDC (Lung) | 50 | none |
| $s_{IDCLN}$[$=\mu_{IDC\_LN}*IDC_{LN}(0)$] | Constant source of IDC (LN) | 50 | none |
| $s_{N4}$ [$=\mu_{N4}*N_4(0)$] | Constant source of N4 (LN) | 5e5 | none |
| $s_{N8}$ [$=\mu_{N8}*N_8(0)$] | Constant source of N8 (LN) | 4.15e5 | none |
| $\mu_{M0}$ | death rate for M0 (lung and LN) | 0.00693 | [1E-3,1E-1] |
| $\mu_{MI}$ | death rate for MI (lung and LN) | 0.014 | [1E-2,1E-1] |
| $\mu_{MA}$ | death rate for M1 (CAM) (lung and LN) | 0.035 | [2E-2,1E-1] |
| $\mu_{M2}$ | death rate for M2 (AAM) (lung and LN) | 0.035 | [1E-2,1E-1] |
| $\mu_{IDC}$ | death rate for IDC | 0.05 | [1E-2,1E-1] |
| $\mu_{MDC}$ | death rate for MDC | 0.3 | [5E-2,5E-1] |
| $\mu_{IDC\_LN}$ | death rate for IDC (LN) | 0.05 | [1E-2,1E-1] |
| $\mu_{MDC\_LN}$ | death rate for MDC (LN) | 0.3 | [5E-2,5E-1] |
| $\mu_{N4}$ | death rate for Naïve CD4+ | 2.5 | [1E-4,1E1] |
| $\mu_{N8}$ | death rate for Naïve CD8+ | 2.5 | [1E-4,1E1] |
| $\mu_{T0}$ | death rate for precursor Th1 | 0.347 | [1E-2,5E-1] |
| $\mu_{T1}$ | death rate for Th1 | 0.55 | [1E-2,2] |
| $\mu_{T8}$ | death rate for T8 | 1 | [1E-2,2] |
| $\mu_{T80}$ | death rate for precursor T8/CTL | 0.347 | [1E-2,5E-1] |
| $\mu_{TC}$ | death rate for CTL | 0.55 | [1E-2,2] |
| $\mu_{TNF}$ | degradation rate for TNF | 2 | [1E-2,5] |
| $\mu_{IG}$ | degradation rate for IFN | 2 | [1E-2,5] |
| $\mu_{I12}$ | degradation rate for IL12 | 2 | [1E-2,5] |
| $\mu_{I10}$ | degradation rate for IL10 | 2 | [1E-2,5] |
| *alpha1* | TNF production rate of MA (Lumg) | 0.01533 | [1E-6,1E3] |
| *chs1* | CFU half-sat on enhancement of TNF production by MA (lung) | 7754.8437 | [1,1E6] |
| *alpha2* | TNF production rate of MI (Lumg) | 6.87E-06 | [1E-6,1E3] |
| *alpha16* | TNF production rate of MDC (Lumg) | 0.00018964 | [1E-6,1E3] |

| | | | |
|---|---|---|---|
| *alpha3* | TNF production rate of CD4+ Ts (Lumg) | 0.001533 | [1E-6,1E3] |
| *alpha4* | TNF production rate of CD8+ Ts (Lumg) | 1.03E-07 | [1E-6,1E3] |
| *chs2* | MA half-sat on enhancement of TNF production by CD8+ Ts (Lung) | 1.0858 | [1,1E6] |
| *sg* | Extra source of IFN: CFU and IL-12 dependent IFN-g production rate (Lung) | 7.2941 | [1E-3,1E2] |
| *chs3* | CFU half-sat on IFN-g production by extra source (Lung) | 21168.0893 | [1,1E6] |
| *chs4* | IL-12 half-sat on IFN-g production by extra source (Lung) | 1E1 | [1E-3,1E2] |
| *alpha5* | IFN-g maximum production rate by Th1 cells (Lung) | 0.00020395 | [1E-6,1E3] |
| *chs5* | MA half-sat on IFN production by Th1 cells (Lung) | 2559.4721 | [1,1E6] |
| *alpha6* | IFN-g maximum production rate by T8 cells (Lung) | 0.0004204 | [1E-6,1E3] |
| *chs6* | MA half-sat on IFN production by T8 cells (Lung) | 3.9454 | [1,1E6] |
| *alpha7* | IFN production rate by MI | 0.0017624 | [1E-6,1E3] |
| *alpha8* | IFN-g maximum production rate by precursor Th1 cells (Lung) | 6.14E-06 | [1E-6,1E3] |
| *chs8* | MDC half-sat on IFN production by precurso Th1 cells (Lung) | 23.324 | [1,1E6] |
| *alpha9* | IFN-g maximum production rate by precursor T8 cells (Lung) | 7.03E-05 | [1E-6,1E3] |
| *chs9* | MDC half-sat on IFN production by precursor T8 cells (Lung) | 8.2004 | [1,1E6] |
| *alpha10* | IL-12 production rate by MDC (Lung) | 2.26E-05 | [1E-6,1E3] |
| *chs10* | IFN half-sat on enhancement of IL12 production by MDC (lung) | 35.2535 | [1E-3,1E2] |
| *alpha11* | IL-12 production rate by MA (Lung) | 8.02E-06 | [1E-6,1E3] |
| *chs11* | IFN half-sat on enhancement of IL12 production by MA (lung) | 2.2915 | [1E-3,1E2] |
| *alpha12* | IL-10 production rate by MAC (Lung) | 4.17E-05 | [1E-6,1E3] |
| *alpha13* | IL-10 production rate by MDC (Lung) | 0.0016125 | [1E-6,1E3] |
| *alpha14* | IL-10 production rate by Th1 cells (Lung) | 1.17E-05 | [1E-6,1E3] |
| *alpha15* | IL-10 production rate by T8 and CTL cells (Lung) | 1.11E-05 | [1E-6,1E3] |
| *chs15* | MA half-sat on enhancement of IL10 production by Ts (Lung) | 1287.9797 | [1,1E6] |
| *alpha17* | IL-10 production rate by M2 (Lung) | 1.09E-05 | [1E-6,1E3] |
| *alpha1a* | TNF production rate of MA (LN) | 5.18E-05 | [1E-6,1E3] |
| *chs1a* | CFU half-sat on enhancement of TNF production by MA (LN) | 10885.3308 | [1,1E6] |
| *alpha2a* | TNF production rate of MI (LN) | 9.81E-05 | [1E-6,1E3] |
| *alpha16a* | TNF production rate of MDC (LN) | 0.00077691 | [1E-6,1E3] |
| *alpha3a* | TNF production rate of CD4+ Ts (LN) | 0.001533 | [1E-6,1E3] |
| *alpha4a* | TNF production rate of CD8+ Ts (LN) | 8.55E-06 | [1E-6,1E3] |
| *chs2a* | MA half-sat on enhancement of TNF production by CD8+ Ts (LN) | 1.035 | [1,1E6] |
| *sgLN* | Extra source of IFN: CFU and IL-12 dependent IFN-g production rate (LN) | 0.092061 | [1E-3,1E2] |
| *chs3a* | CFU half-sat on IFN-g production by extra source (LN) | 6348149.912 | [1,1E6] |
| *chs4a* | IL-12 half-sat on IFN-g production by extra source (LN) | 84589.7348 | [1E-3,1E2] |
| *alpha5a* | IFN-g maximum production rate by Th1 cells (LN) | 7.12E-06 | [1E-6,1E3] |
| *chs5a* | MA half-sat on IFN production by Th1 cells (LN) | 5.8983 | [1,1E6] |
| *alpha6a* | IFN-g maximum production rate by T8 cells (LN) | 0.0020684 | [1E-6,1E3] |
| *chs6a* | MA half-sat on IFN production by T8 cells (LN) | 4.268 | [1,1E6] |
| *alpha7a* | IFN production rate by MI | 0.0010406 | [1E-6,1E3] |
| *alpha8a* | IFN-g maximum production rate by precursor Th1 cells (LN) | 2.95E-06 | [1E-6,1E3] |
| *chs8a* | MDC half-sat on IFN production by precurso Th1 cells (LN) | 1970.2791 | [1,1E6] |
| *alpha9a* | IFN-g maximum production rate by precursor T8 cells (LN) | 0.0012697 | [1E-6,1E3] |
| *chs9a* | MDC half-sat on IFN production by precurso T8 cells (LN) | 269.7575 | [1,1E6] |
| *alpha10a* | IL-12 production rate by MDC (LN) | 0.23205 | [1E-6,1E3] |
| *chs10a* | IFN half-sat on enhancement of IL12 production by MDC (LN) | 26.8302 | [1E-3,1E2] |
| *alpha11a* | IL-12 production rate by MA (LN) | 0.010636 | [1E-6,1E3] |
| *chs11a* | IFN half-sat on enhancement of IL12 production by MA (LN) | 98.7184 | [1E-3,1E2] |

| | | | |
|---|---|---|---|
| *alpha12a* | IL-10 production rate by MAC (LN) | 0.0046598 | [1E-6,1E3] |
| *alpha13a* | IL-10 production rate by MDC (LN) | 0.00094216 | [1E-6,1E3] |
| *alpha14a* | IL-10 production rate by Th1 cells (LN) | 1.26E-05 | [1E-6,1E3] |
| *alpha15a* | IL-10 production rate by T8 and CTL cells (LN) | 2.30E-06 | [1E-6,1E3] |
| *chs15a* | MA half-sat on enhancement of IL10 production by Ts (LN) | 272.2163 | [1,1E6] |
| *alpha17a* | IL-10 production rate by M2 (LN) | 0.003521 | [1E-6,1E3] |

**Table S3**: list of all the non-zero initial conditions for the 32 equations ODE system. Measure units are number of cells in the whole organ (lung or lymph node). Bacterial infection is introduced after homeostasis is reached, i.e. with $M_2$ initial conditions set to the values below.

| Variable | Lung | Lymph Node |
|---|---|---|
| Undifferentiated Macrophages [$M_0$] | 2e3 | 5e2 |
| Alternatively Activated Macrophages [$M_2$] | 5.713e3 | 1.4283e3 |
| Immature Dendritic Cells [IDC] | 1e3 | 1e3 |
| Naïve Lymphocytes[$N_4$ and $N_8$] | | CD4 = 2e5<br>CD8 = 0.8*2e5 |

**Table S4**: US analysis results for the LHS2 experiment. In parenthesis is the PRCC value. The correlation index is Partial Rank Correlation Coefficient (PRCC). In this context, a positive impact of a particular mechanism on a specific output (positive PRCC) means that if that mechanism is increased/enhanced, the output will likely increase, or vice versa. On the other hand, a negative impact (negative PRCC) is when an increase in a specific mechanism results in a decrease in the output, and vice versa. There is a strict criteria for significance ($p<1e-3$) and we only show PRCC>±0.15. The outputs are correlated after 100 days post infection. *: only significant within 2 weeks post infection.

| Output | Positive Correlation | Negative correlation |
|---|---|---|
| $M_l$ in the Lung | $rc_2$ (0.25), $k_7$ (0.4), $k_1$ (0.3), CFUlung* | $k_5$ (-0.3) |
| $M_l$ in the LN | $rc_{2a}$ (0.33), $k_{7a}$ (0.3), $k_{1a}$ (0.5) | $k_{5a}$ (-0.4) |
| CAM in the Lung | $k_2$ (0.5), $rc_2$ (0.39), $hs_{l10}$ (0.2), $rc_1$ (0.32), | $k_5$ (-0.33) $hs_2$ (-0.2), |
| CAM in the LN | $k_{2a}$ (0.5), $rc_{2a}$ (0.43), $hs_{l10a}$ (0.24) , $rc_{1a}$ (0.22), | $k_{5a}$ (-0.28), $hs_{2a}$ (-0.18), $hs_{3a}$ (-0.3) |
| AAM in the Lung | $k_7$ (0.5), $rc_2$ (0.36), $rc_1$ (0.25) | $k_5$ (-0.35), $k_1$ (-0.47), $hs_{l10}$ (-0.15) |
| AAM in the LN | $k_{7a}$ (0.6), $rc_{2a}$ (0.55), $rc_{1a}$ (0.32) | $k_{5a}$ (-0.52), $k_{1a}$ (-0.3) |
| MDC in the Lung | $k_{12}$ (0.18), $rc_4$ (0.35), $hs_{l10\text{-}DC}$* (0.3) , CFUlung* | |
| MDC in the LN | $k_{12}$* (0. 5), $hs_{l10\text{-}DCLN}$ (0.3), $k_{12a}$ (0.2), CFUlung* | scaling* (-0.2) |
| MPF in the Lung | $hs_{l10}$ (0.3), $k_1$* (0.2), CFUlung* | $hs_2$ (-0.3), $rc_4$ (-0.23), $k_2$ (-0.18) |
| MPF in the LN | $hs_{l10a}$ (0.3) | $hs_{2a}$ (-0.2), $hs_{3a}$ (-0.35), $\xi_1$ (-0.15), $k_{2a}$ (-0.18) |
| Switching time in the Lung | $k_7$ (0.4), $hs_2$ (0.27) | $k_2$ (-0.55), $hs_{l10}$ (-0.22), $k_1$ (-0.15), $k_{15}$ (-0.18), $rc_2$ (-0.18) |
| Switching time in the LN | $k_{7a}$ (0.48), $hs_{3a}$ (0.23) | $k_{2a}$ (-0.45), $hs_{l10a}$ (-0.2), $k_{5a}$ (-0.22) |

**References**


1. Demangel C, Bertolino P, Britton WJ (2002) Autocrine IL-10 impairs dendritic cell (DC)-derived immune responses to mycobacterial infection by suppressing DC trafficking to draining lymph nodes and local IL-12 production. Eur J Immunol 32: 994-1002.
2. Obregon C, Rothen-Rutishauser B, Gitahi SK, Gehr P, Nicod LP (2006) Exovesicles from human activated dendritic cells fuse with resting dendritic cells, allowing them to present alloantigens. Am J Pathol 169: 2127-2136.
3. Smith CM, Wilson NS, Waithman J, Villadangos JA, Carbone FR, et al. (2004) Cognate CD4(+) T cell licensing of dendritic cells in CD8(+) T cell immunity. Nat Immunol 5: 1143-1148.
4. Thery C, Duban L, Segura E, Veron P, Lantz O, et al. (2002) Indirect activation of naive CD4+ T cells by dendritic cell-derived exosomes. Nat Immunol 3: 1156-1162.
5. Einarsdottir T, Lockhart E, Flynn JL (2009) Cytotoxicity and secretion of gamma interferon are carried out by distinct CD8 T cells during Mycobacterium tuberculosis infection. Infect Immun 77: 4621-4630.
6. Lucey DR, Clerici M, Shearer GM (1996) Type 1 and type 2 cytokine dysregulation in human infectious, neoplastic, and inflammatory diseases. Clin Microbiol Rev 9: 532-562.
7. Barnes PF, Lu S, Abrams JS, Wang E, Yamamura M, et al. (1993) Cytokine production at the site of disease in human tuberculosis. Infect Immun 61: 3482-3489.
8. Tsukaguchi K, de Lange B, Boom WH (1999) Differential regulation of IFN-gamma, TNF-alpha, and IL-10 production by CD4(+) alphabetaTCR+ T cells and vdelta2(+) gammadelta T cells in response to monocytes infected with Mycobacterium tuberculosis-H37Ra. Cell Immunol 194: 12-20.
9. Giacomini E, Iona E, Ferroni L, Miettinen M, Fattorini L, et al. (2001) Infection of human macrophages and dendritic cells with Mycobacterium tuberculosis induces a differential cytokine gene expression that modulates T cell response. J Immunol 166: 7033-7041.
10. Chensue SW, Ruth JH, Warmington K, Lincoln P, Kunkel SL (1995) In vivo regulation of macrophage IL-12 production during type 1 and type 2 cytokine-mediated granuloma formation. J Immunol 155: 3546-3551.
11. Fulton SA, Johnsen JM, Wolf SF, Sieburth DS, Boom WH (1996) Interleukin-12 production by human monocytes infected with Mycobacterium tuberculosis: role of phagocytosis. Infect Immun 64: 2523-2531.
12. Fulton SA, Cross JV, Toossi ZT, Boom WH (1998) Regulation of interleukin-12 by interleukin-10, transforming growth factor-beta, tumor necrosis factor-alpha, and interferon-gamma in human monocytes infected with Mycobacterium tuberculosis H37Ra. J Infect Dis 178: 1105-1114.
13. Martinez FO, Sica A, Mantovani A, Locati M (2008) Macrophage activation and polarization. Front Biosci 13: 453-461.
14. Moore KW, de Waal Malefyt R, Coffman RL, O'Garra A (2001) Interleukin-10 and the interleukin-10 receptor. Annu Rev Immunol 19: 683-765.